Elsevier Editorial System(tm) for Chemosphere

Manuscript Draft

Manuscript Number: CHEM57356R1

Title: Adsorption of Methyl tert-butyl ether (MTBE) onto ZSM-5 zeolite: Fixed-bed column tests, breakthrough curve modelling and regeneration

Article Type: Research paper

Section/Category: Treatment and Remediation

Keywords: MTBE, ZSM-5 zeolite, Fixed-bed column tests, Permeable reactive barriers, Regeneration

Corresponding Author: Miss Yunhui Zhang,

Corresponding Author's Institution: University of Cambridge

First Author: Yunhui Zhang

Order of Authors: Yunhui Zhang; Fei Jin, PhD; Zhengtao Shen, PhD; Fei Wang, PhD; Rod Lynch, PhD; Abir Al-Tabbaa, PhD

Abstract: ZSM-5, as a hydrophobic zeolite, has a good adsorption capacity for methyl tert-butyl ether (MTBE) in batch adsorption studies. This study explores the applicability of ZSM-5 as a reactive material in permeable reactive barriers (PRBs) to decontaminate the MTBE-containing groundwater. A series of laboratory scale fixed-bed column tests were carried out to determine the breakthrough curves and evaluate the adsorption performance of ZSM-5 towards MTBE under different operational conditions, including bed length, flow rate, initial MTBE concentration and ZSM-5 dosage, and regeneration tests were carried out at 80, 150 and 300°C for 24 h. Dose-Response model was found to best describe the breakthrough curves. MTBE was effectively removed by the fixed-bed column packed with a ZSM-5/sand mixture with an adsorption capacity of 31.85 mg·g-1 at 6 cm bed length, 1 mL·min-1 flow rate, 300 mg·L-1 initial MTBE concentration and 5% ZSM-5 dosage. The maximum adsorption capacity increased with the increase of bed length and the decrease of flow rate and MTBE concentration. The estimated kinetic parameters can be used to predict the dynamic behaviour of column systems. In addition, regeneration study shows that the adsorption capacity of ZSM-5 remains satisfactory (>85%) after up to four regeneration cycles.

Adsorption of Methyl tert-butyl ether (MTBE) onto ZSM-5 zeolite: Fixed-bed column tests, breakthrough curve modelling and regeneration

Yunhui Zhang[a]; Fei Jin[b]; Zhengtao Shen[c]; Fei Wang[d]; Rod Lynch[a]; Abir Al-Tabbaa[a]*

[a]Department of Engineering, University of Cambridge, Cambridge, CB2 1PZ, United Kingdom

[b]School of Engineering, University of Glasgow, Glasgow, G12 8QQ, United Kingdom

[c]Department of Earth and Atmospheric Sciences, University of Alberta, Edmonton T6G 2E3, Canada

[d]Institute of Geotechnical Engineering, School of Transportation, Southeast University, Nanjing, 210096, China

AUTHOR INFORMATION

***Corresponding Author**

Tel: +44- (0) 7821464199

E-mail address: yz485@cam.ac.uk.

Abstract

ZSM-5, as a hydrophobic zeolite, has a good adsorption capacity for methyl tert-butyl ether (MTBE) in batch adsorption studies. This study explores the applicability of ZSM-5 as a reactive material in permeable reactive barriers (PRBs) to decontaminate the MTBE-containing groundwater. A series of laboratory scale fixed-bed column tests were carried out to determine the breakthrough curves and evaluate the adsorption performance of ZSM-5 towards MTBE under different operational conditions, including bed length, flow rate, initial MTBE concentration and ZSM-5 dosage, and regeneration tests were carried out at 80, 150 and 300 °C for 24 h. Dose-Response model was found to best describe the breakthrough curves. MTBE was effectively removed by the fixed-bed column packed with a ZSM-5/sand mixture with an adsorption capacity of 31.85 $mg \cdot g^{-1}$ at 6 cm bed length, 1 $mL \cdot min^{-1}$ flow rate, 300 $mg \cdot L^{-1}$ initial MTBE concentration and 5% ZSM-5 dosage. The maximum adsorption capacity increased with the increase of bed length and the decrease of flow rate and MTBE concentration. The estimated kinetic parameters can be used to predict the dynamic behaviour of column systems. In addition, regeneration study shows that the adsorption capacity of ZSM-5 remains satisfactory (>85%) after up to four regeneration cycles.

Key words: MTBE, ZSM-5 zeolite, Fixed-bed column tests, Permeable reactive barriers, Regeneration

1. Introduction

Gasoline spills from the accidental leakage of storage tanks, transfer pipes and boats are typical pollution sources of soil, groundwater, surface water and the marine environment (Reuter et al., 1998). Methyl tert-butyl ether (MTBE) was an extensively used gasoline additive for fuel oxygenation. In spite of the bans in some countries, it is still the second most common volatile organic compound in shallow groundwater (Levchuk et al., 2014). Due to its genotoxicity, its hazard of causing skin and eye irritation and its unpleasant odour (Mancini et al., 2002), the existence of MTBE in aquatic environments has raised considerable public concerns.

Permeable reactive barriers (PRBs) is an effective in-situ technology for aquifer and groundwater remediation (Hou et al., 2014). Due to the rapid migration (Levchuk et al., 2014) and limited natural biodegradation potential of MTBE (Lindsey et al., 2017; Mohebali, 2013), using PRBs to mitigate/eliminate MTBE contamination holds much promise. As the key component of PRBs, the reactive medium is selected primarily depending on the nature of target contaminants and the hydro-geological conditions of field sites. ZSM-5 as a reactive medium in the PRBs can act as adsorbents due to its high adsorption capacity (Abu-Lail et al., 2010; Martucci et al., 2015; Zhang et al., 2018b) and hydrogen form of ZSM-5 (HZSM-5) may also catalyse the hydrolysis of MTBE to *t*-butyl alcohol (TBA) and methanol which are more biodegradable (Centi et al., 2002; Knappe and Campos, 2005). These products can also be adsorbed onto ZSM-5 and be released slowly with time which favours their biodegradation by microorganisms growing on the barrier (Centi and Perathoner, 2003). The PRBs design requires a kinetic characterisation using fixed-bed columns as a simulation of real PRBs to evaluate the dynamic removal of contaminants for the practical application (Cruz Viggi et al., 2010; Gavaskar, 1999). Various theoretical models, such as Logit, Adams-

Bohart, Thomas, Yoon and Nelson, Dose and Response, and bed length/service time (BDST) models, have been developed to fit the experimental data and obtain the breakthrough curves and column kinetic parameters. These parameters can be employed to predict the adsorption performance under new operational conditions and further facilitate the full-scale design of fixed-bed column systems, e.g., PRBs.

To date, fixed-bed column tests have been widely applied to simulate PRBs towards various contaminants, such as heavy metals and dyes (Calero et al., 2009; Han et al., 2008), with different adsorbents such as activated carbon and zeolites (García-Mateos et al., 2015; Ozdemir et al., 2009) etc. Nevertheless, to our best knowledge, limited studies exist on fixed-bed column tests of using ZSM-5 for MTBE removal, especially regarding the influence of operational conditions, such as the bed length, flow rate, inlet adsorbate concentrations and the percentage of the adsorbent on the adsorption behaviour. Abu-Lail et al. (2010) studied the removal of MTBE with three adsorbents including granular ZSM-5 in large and small diameter fixed-bed columns, and evaluated the influence of bed length on the breakthrough curves with the BDST model. It was shown that the granular ZSM-5 with a shorter bed length reached the breakthrough point earlier due to the less mass of adsorbents in the column. However, besides the bed length, other variables, such as flow rate, the MTBE concentration and ZSM-5 dosage, also need to be considered in practical groundwater contamination applications due to the fact that the groundwater flow rate and MTBE concentrations vary in different regions. Therefore, this study discussed the influence of several operational parameters (bed length, flow rate, initial MTBE concentration and ZSM-5 percentage) in fixed-bed column tests. The parameters obtained from modelling are crucial for PRB design and can be used to guide the application of ZSM-5 as a reactive medium in the PRBs for the MTBE-contaminated groundwater remediation.

Reusability is considered as a key criterion to judge the feasibility of an adsorbent in practical applications (Xin et al., 2017). The exhausted adsorbents are generally considered as hazardous wastes and need to be incinerated, leading to secondary pollution, such as thermal pollution and potential desorption of adsorbate in the atmosphere (Shah et al., 2014). The regeneration of spent adsorbents can recover material resources, minimize the demands of virgin adsorbents and avoid the generation of hazardous waste. Zeolites, including ZSM-5, demonstrate good stability under a wide range of environmental conditions, such as acidic (Pascoe, 1992) and high temperature environments (Anderson, 2000). They can be regenerated by heat treatment, chemical treatment, such as Fenton oxidation (Wang and Zhu, 2006) and KCl (Katsou et al., 2011), and biological regeneration (Wei et al., 2011). However, chemical or biological methods may lead to the generation of hazardous residues. Although HZSM-5 may adsorb and catalyse the hydrolysis of MTBE, and then release the adsorbed reaction products (TBA and methanol) to achieve self-regeneration, this process takes a long time (Centi and Perathoner, 2003) and our previous study showed that the desorption was negligible after 3 days in batch tests (Zhang et al., 2018b). Further studies will investigate the long term behaviour. Thermal regeneration is effective and time-saving for adsorbents used for volatile and semi-volatile organic compounds, including MTBE, due to its high vapour pressure under normal temperatures and low boiling points. In this study, in order to avoid excessive consumption of materials and secondary pollution, repeated thermal regeneration was used for the regeneration of ZSM-5 to evaluate the stability of ZSM-5 after several adsorption-desorption cycles.

This study aims to (1) analyse the effects of various operational conditions (flow rate, bed length, initial MTBE concentration and ZSM-5 percentage) in fixed-bed column tests on the

MTBE adsorption onto ZSM-5; (2) find the most suitable model to describe the breakthrough curve and obtain column parameters; (3) predict adsorption performance at a new flow rate without further experimental runs with the BDST model and (4) examine the recyclability of ZSM-5 with repeated thermal regeneration tests.

2. Materials and methods

2.1 Materials

MTBE was purchased from Fisher Scientific, and hydrogen form of ZSM-5 powder was obtained from Acros Organics. ZSM-5 used in this study has a large surface area of 400 $m^2 \cdot g^{-1}$ and a high SiO_2/Al_2O_3 ratio of 469. Two pore systems, i.e. zig-zag channels and straight channels, exist in the structure of ZSM-5 with pore sizes of 5.3×5.6 Å and 5.1×5.5 Å, respectively. The detailed physicochemical properties and framework structure of ZSM-5 can be found in (Zhang et al., 2018b).

2.2 Fixed-bed column tests

A series of fixed-bed column tests were conducted in a Pyrex glass column (2 cm inner diameter and 10 cm high) for the simulation of ZSM-5 containing PRBs for MTBE adsorption. There is a layer of glass beads and a stainless steel mesh filter attached to each end of the column to ensure the uniform flow of the solution. The schematic of the fixed-bed column set-up is shown in Figure 1.

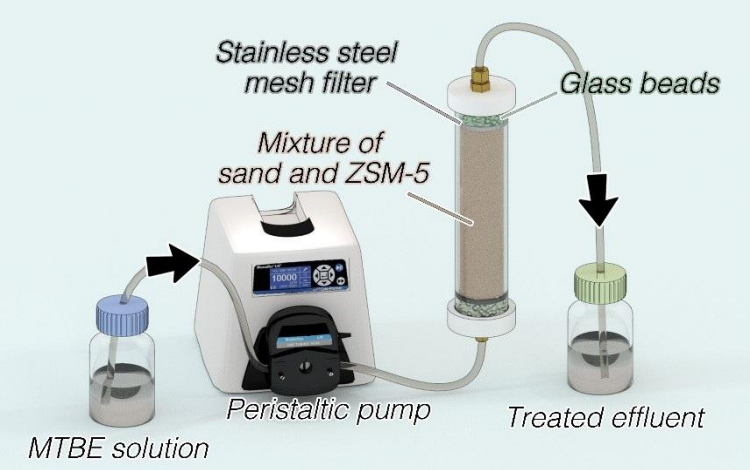

Figure 1 The schematic of the fixed-bed column set-up in this study

ZSM-5 was mixed with sand to increase the permeability due to the fine texture of ZSM-5 (Cappai et al., 2012). Columns were filled with a mixture of ZSM-5 (5% or 10% in w/w of sand) and sand to produce different bed lengths (3, 6 and 9 cm). The initial water content of the specimen was designated as 10% in w/w (of sand) and the bulk density was about 2 $g \cdot cm^{-3}$. The values of hydraulic conductivity of the mixture in the column were measured as 6.32 $\times 10^{-6}$ $m \cdot s^{-1}$ (5% ZSM-5 and sand) and 1.21 $\times 10^{-6}$ $m \cdot s^{-1}$ (10% ZSM-5 and sand). It was assumed that the specific gravity values of sand and ZSM-5 were 2.65 and 2 respectively in this study (Jha and Singh, 2016; Masad et al., 1996). It is noted that the seepage velocity differs at different regions and different depths (Gavaskar et al., 2000). Therefore in this study, pump rate (i.e., seepage rate) was selected based on a previous land remediation project with sandy soils in the ground (Al-Tabbaa and Liska, 2012). The solutions with different MTBE concentrations (200, 300 and 400 $mg \cdot L^{-1}$) were pumped upward at different flow rates of 0.5 $mL \cdot min^{-1}$ (seepage velocity: 0.011 $cm \cdot s^{-1}$), 1 $mL \cdot min^{-1}$ (seepage velocity: 0.022 $cm \cdot s^{-1}$) and 2 $mL \cdot min^{-1}$ (seepage velocity: 0.044 $cm \cdot s^{-1}$) controlled by a peristaltic pump. Flow rates and MTBE concentrations in this study were higher than the actual conditions in

most regions to save the operational time in the lab. Also, the PRBs were generally installed near pollution sources with a high MTBE concentration.

The detailed operation variables are listed in Table 1. Where m_{ZSM-5} is the mass of ZSM-5 in the column (g). The effect of flow rate was studied by tests C, F0.5 and F2; the effect of bed length was examined by tests C, B3 and B9; tests C and Z10 were conducted to discuss the effect of ZSM-5 dosage and tests C, M200 and M400 ascertained the effect of initial MTBE concentration. The effluents at the outlet were collected at set intervals and the MTBE concentration was measured. The saturation time (t_s) was established when the effluent MTBE concentration exceeded 85% of inlet concentration. The breakthrough time (t_b) (Goel et al., 2005) is established when the effluent MTBE concentration reaches 5% of the inlet concentration (C/C_0=0.05) (García-Mateos et al., 2015).

Table 1 Operational variables for fixed-bed column tests

Test No.	Influencing factors	Flow rate ($mL \cdot min^{-1}$)	Bed length (cm)	m_{ZSM-5} (g)	ZSM-5 (%)	C_0 (MTBE) ($mg \cdot L^{-1}$)	Porosity
F0.5	Flow rate	0.5	6	2.05	5	300	0.25
C	Flow rate	1	6	2.05	5	300	0.24
F2	Flow rate	2	6	2.05	5	300	0.24
B3	Bed length	1	3	1.03	5	300	0.24
C	Bed length	1	6	2.05	5	300	0.24
B9	Bed length	1	9	3.08	5	300	0.24
C	ZSM-5 dosage	1	6	2.05	5	300	0.24
Z10	ZSM-5 dosage	1	6	4.50	10	300	0.23

M200	MTBE concentration	1	6	2.07	5	200	0.24
C	MTBE concentration	1	6	2.05	5	300	0.24
M400	MTBE concentration	1	6	2.03	5	400	0.25

168

169 2.3 Regeneration cycles

170 The thermal regeneration tests were conducted to examine the recyclability of ZSM-5 at
171 different temperatures based on batch adsorption tests. After MTBE adsorption in aqueous
172 solution with ZSM-5, the saturated ZSM-5 was heated at 80, 150 or 300 °C for 24 h in a
173 muffle furnace (Carbolite CWF 1200, UK), and then 0.1 g of regenerated ZSM-5 was added
174 to 20 mL 300 $mg \cdot L^{-1}$ of MTBE solution for adsorption for 24h. After each regeneration cycle,
175 the MTBE removal percentage was determined and this process was repeated up to 6 times.

176

177 2.4 Analytical methods

178 MTBE concentration was analysed by an ambient headspace technique as described in our
179 previous studies (Chan and Lynch, 2003; Zhang et al., 2018b) using a gas chromatograph
180 (Agilent 6850 Series) with a flame ionisation detector (GC-FID). Each headspace sample was
181 measured in triplicate. Data fitting and modelling was performed by OriginPro 8.5 software.
182 The values of Akaike information criterion (AIC) and correlation coefficient (R^2) were used
183 to compare different models. The lower AIC and higher R^2 values indicate a more suitable
184 model.

185

186 2.5 Mathematical models for breakthrough curves

The operational parameters, such as the breakthrough time, saturation time, the shape of breakthrough curves and the column adsorption capacity, play important roles in the evaluation of the operational and adsorption performance of columns. They can be obtained from a plot of C/C_0 against time (t) using the non-linear regression method. Several mathematical models, such as Adams-Bohart model, the Logit method, Thomas model, Yoon-Nelson model and Dose-Response model, have been developed and widely applied to fit the experimental data of column tests to predict the concentration-time profiles and breakthrough curves. Therefore, these models were used in this study to find the most suitable model to describe the breakthrough curve and obtain maximum column capacity. This will help avoid unnecessary investment and high operational costs in the design and operation of a full-scale column caused by possible underutilized or oversaturated columns.

2.5.1 Adams-Bohart model

The Adams-Bohart model (Bohart and Adams, 1920) was developed based on the assumption that adsorption rate is proportional to the adsorbent's residual capacity and the adsorbate's concentration (Goel et al., 2005). It is generally used to describe the initial portion ($C/C_0<0.15$) of the breakthrough curve and has been extensively applied in other various systems (Calero et al., 2009; Sağ and Aktay, 2001). The expression is given as follows

$$\frac{C}{C_0} = \frac{e^{k_{AB}C_0 t}}{e^{(k_{AB}N_0 Z/v)} - 1 + e^{k_{AB}C_0 t}} \quad (1)$$

where k_{AB} is the rate constant ($L \cdot mg^{-1} \cdot min^{-1}$) and N_0 is the volumetric adsorption capacity ($mg \cdot L^{-1}$).

2.5.2 Bed depth/service time (BDST) model

BDST model (Oulman, 1980) is rearranged from the Adams-Bohart model by Hutchins (Hutchins, 1973) to produce a linear relationship between the bed length (Z, cm) and service time (t, min). It is based on the assumption that the moving speed of the adsorption zone in the column is constant, and can be described as follows:

$$t = \frac{N_0}{C_0 v} Z - \frac{1}{C_0 k_{AB}} \ln\left(\frac{C_0}{C} - 1\right) \quad (2)$$

$$a = \frac{N_0}{C_0 v} \quad (3)$$

$$b = \frac{1}{C_0 k_{AB}} \ln\left(\frac{C_0}{C} - 1\right) \quad (4)$$

The values of N_0 and k_{AB} can be obtained from a plot of Z against t. The advantage of the BDST model is that only three column tests are required to collect the experimental data (Adak and Pal, 2006; Hutchins, 1973).

For a new operational condition, such as a new linear flow rate (v'), the new slope (a') and intercept (b') can be calculated directly by Equation (5) and (6), respectively.

$$a' = a\frac{v}{v'} \quad (5)$$

$$b' = b \quad (6)$$

2.5.3 Logit method

BDST model may cause errors if the service time at which the effluent exceeds the breakthrough criteria was selected. Therefore, Logit method was established to provide a rational basis for the fitting to the data and the reduction of errors (Oulman, 1980).

The equation of the Logit method (Oulman, 1980) can be written as

$$ln\left(\frac{\frac{C}{C_0}}{1-\frac{C}{C_0}}\right) = KC_0 t - \frac{KNZ}{v} \quad (7)$$

To apply it to describe the breakthrough curve, Equation (7) is rearranged as

$$\frac{C}{C_0} = \frac{e^{(KC_0 t - KNZ/v)}}{1+e^{(KC_0 t - KNZ/v)}} \quad (8)$$

where v is the linear flow rate ($cm \cdot min^{-1}$), C is the solute concentration ($mg \cdot L^{-1}$), C_0 is the inlet MTBE concentration ($mg \cdot L^{-1}$), K is the adsorption rate coefficient ($L \cdot mg^{-1} \cdot min^{-1}$) and N is the adsorption capacity coefficient ($mg \cdot L^{-1}$).

2.5.4 Thomas model

Thomas model (Equation (9)) based on the mass-transfer theory and was used to calculate the maximum adsorption capacity (q_0, $mg \cdot g^{-1}$) and the Thomas adsorption rate constant (K_{Th}, $L \cdot mg^{-1} \cdot min^{-1}$) using experimental data from fixed-bed column tests (Thomas, 1944, 1948).

$$\frac{C}{C_0} = \frac{1}{1+e^{\frac{k_{Th}}{Q}(q_0 m - C_0 V)}} \quad (9)$$

where V is the effluent volume (L), m is the mass of adsorbent (g), and Q is the flow rate of the influent ($L \cdot min^{-1}$).

2.5.5 Yoon and Nelson model

The wide use of Yoon and Nelson model (Yoon, 1984) in single adsorbate systems is attributed to its simplicity since no detailed data is needed regarding the properties of adsorbate, adsorbent and the column. The equation is given by:

$$\frac{C}{C_0} = \frac{1}{1+e^{k_{YN}(\tau - t)}} \quad (10)$$

where τ is the time required for 50% adsorbate breakthrough (min) and k_{YN} is the rate constant (min^{-1}). This model assumes that the declining rate in the probability of adsorption is proportional to that of both adsorbate adsorption and adsorbate breakthrough on the adsorbent (Ayoob and Gupta, 2007).

2.5.6 Dose-Response model

Dose-Response model (Yan et al., 2001) is an empirical model and has been widely used to describe the column kinetics and behaviour, especially heavy metal removal (Dorado et al., 2014). The general equation is as follows:

$$\frac{C}{C_0} = 1 - \frac{1}{1+(\frac{C_0 V}{q_0 m})^a} \quad (11)$$

$$b = V_{(50\%)} = \frac{q_0 m}{C_0} \quad (12)$$

where a is the constant, b is equal to $V_{(50\%)}$, the concentration when 50% of the maximum response occurs (L).

3. Results and discussion

3.1 Breakthrough curve modelling

The concentration-time profiles were obtained after a series of fixed-bed column experiments. Five models were applied to fit the experimental data to describe the fixed-bed column behaviour. The empirical Dose-Response model best described the experimental data in different column conditions (R^2>0.95 with the lowest AIC value), suggesting its suitability to be used for the design and scale-up purpose. This model was also shown to reduce the errors of two conventional mathematical models, i.e. Thomas model and Adams-Bohart model, for the biosorption of heavy metals in a column (Yan et al., 2001). The fitting results of the Dose-Response model are shown in Table 2 and those of other models are shown in Table S1 and Figure S1-S4 in the Appendix.

From Table 2, the values of q_0 increased with the increase of bed length and the decrease of flow rate, ZSM-5 dosage and initial MTBE concentration. The adsorption capacity (q_0) was calculated as 26.32 $mg \cdot g^{-1}$ at 6 cm bed length, 1 $mL \cdot min^{-1}$ flow rate, 300 $mg \cdot L^{-1}$ initial MTBE concentration and 5% ZSM-5 dosage (Test No. C).

Table 2 Dose-Response model parameters for the MTBE adsorption on ZSM-5 under different operational conditions

Variables	Test No.	a	b (mL)	q_0 ($mg \cdot g^{-1}$)	R^2
Flow rate	C	1.84	179.88	26.32	0.993
	F0.5	3.14	213.16	31.19	0.997
	F2	0.95	90.99	13.32	0.959
Bed length	C	1.84	179.88	26.32	0.993
	B3	1.06	43.46	12.66	0.997

	B9	3.14	294.63	28.70	0.991
ZSM-5 percentage	C	1.84	179.88	26.32	0.993
	Z10	1.45	280.78	18.72	0.971
Initial MTBE	C	1.84	179.88	26.32	0.993
concentration	M200	1.67	232.38	22.45	0.989
	M400	1.23	107.34	21.15	0.969

277

278 3.2 Column parameters calculation

279 The column adsorption capacity of the adsorbent is a critical indicator of column
280 performance and could be calculated from the breakthrough curve. Considering the best
281 fitting results of the Dose-Response model in Session 3.1, all the breakthrough parameters
282 under certain operational conditions were calculated based on the Dose-Response model
283 fitting and are listed in Table 3. Where MTZ is the length of the mass transfer zone (cm),
284 m_{adsorb} is the adsorbed amount of MTBE (mg), m_{total} is the total amount of MTBE through the
285 column (mg), q_e is the equilibrium MTBE uptake, also called column maximum separation
286 capacity ($mg \cdot g^{-1}$) (Gouran-Orimi et al., 2018), C_e is the equilibrium MTBE concentration
287 ($mg \cdot L^{-1}$), and R is the total MTBE removal percentage (%).

288

289 It is obvious that both the breakthrough time and saturation time increased with the
290 decreasing flow rate and initial MTBE concentration. The same trend was shown when the
291 bed length or ZSM-5 dosage were increased. The maximum column separation capacity is
292 31.85 $mg \cdot g^{-1}$ at 6 cm bed length, 1 $mL \cdot min^{-1}$ flow rate, 300 $mg \cdot L^{-1}$ initial MTBE
293 concentration and 5% ZSM-5 dosage (Test No. C) in this study. In comparison, the maximum
294 adsorption capacity in batch adsorption tests were calculated as 53.55 $mg \cdot g^{-1}$ in our previous
295 study (Zhang et al., 2018b), which almost doubled that in fixed-bed column tests (31.85

296 mg·g^{-1}). This is mainly due to the insufficient contact time between ZSM-5 and MTBE in
297 columns (461 min and 24 h for column tests and batch tests, respectively). It should be noted
298 that both the adsorption capacity (q_0 in Table 2) and the maximum column separation
299 capacity (q_e in Table 3) decreased with a higher ZSM-5 percentage in spite of a higher
300 adsorbed amount of MTBE (m_{adsorb} in Table 3). This may be explained by the phenomenon
301 that ZSM-5 was easier to run away with the MTBE flow with a higher ZSM-5 dosage,
302 leading to an underestimate of the adsorption capacity, which is a limitation of this study.
303
304 Table 3 Parameters of breakthrough curves for MTBE adsorption on ZSM-5 in fixed-bed
305 columns under different operational conditions

Test No.	C	F0.5	F2	B3	B9	Z10	M200	M400
t_b (min)	36.77	167.87	2.08	2.86	115.28	36.84	40.29	10.13
t_s (min)	460.81	740.18	260.00	220.00	512.25	919.75	655.79	442.04
$MTZ = \frac{Z(t_s - t_b)}{t_s}$ (cm)	5.52	4.64	5.95	2.96	6.97	5.76	5.63	5.86
$m_{adsorb} = \frac{Q}{1000}\int_{t=0}^{t=t_{total}}(C_0 - C)dt$ (mg)	65.30	67.42	52.99	23.01	93.23	114.99	52.77	66.52
$m_{total} = \frac{C_0 Q t_{total}}{1000}$ (mg)	138.24	111.03	156.00	66.00	153.68	275.93	131.16	176.82
$q_e = \frac{m_{adsorb}}{m_{zsm-5}}$ (mg·g^{-1})	31.85	32.89	25.85	22.34	30.27	25.55	25.49	32.77
$C_e = \frac{1000(m_{total} - m_{adsorb})}{Q t_{total}}$ (mg·L^{-1})	158.29	117.82	198.10	195.42	118.00	174.98	119.53	249.52
$R = \frac{100 m_{adsorb}}{m_{total}}$ (%)	47.24	60.73	33.97	34.86	60.67	41.67	40.23	37.62

306

3.3 Influence of operational conditions on MTBE removal

3.3.1 Effect of flow rate

Figure 2 shows the breakthrough curves at different flow rates of 0.5, 1 to 2 mL·min^{-1} in relation to pore volume and service time. As shown in Figure 2, the plots were closer to a classic S-shaped breakthrough curve at a lower flow rate (0.5 mL·min^{-1}), indicating a slower process and a higher adsorption capacity (32.89 mg·g^{-1}).

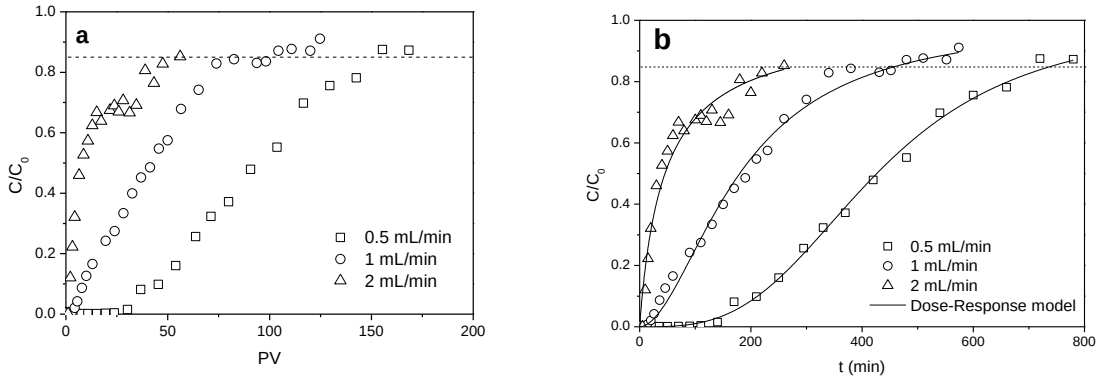

Figure 2 Breakthrough curves at different flow rates as a function of (a) pore volume (PV) and (b) time (t). (C_0=300 mg·L^{-1}, bed length=6 cm, ZSM-5 dosage=5%)

As the flow rate increased from 0.5 mL·min^{-1} to 2 mL·min^{-1}, the breakthrough time and saturation time decreased from 167.87 min to 2.08 min and from 740.18 min to 260.00 min, respectively. A lower column adsorption capacity was obtained at 25.85 mg·g^{-1} as shown in Table 3. This is due to the fact that the movement of MTBE is accelerated with an increase in the flow rate, which could cause insufficient residence time of MTBE in the column (Ozdemir et al., 2009; Salman et al., 2011). Similar agreement was found for the adsorption of nitrate on bio-inspired polydopamine coated zeolite and was explained by low residency in the column at high flow rate (Gouran-Orimi et al., 2018).

3.3.2 Effect of bed length

The breakthrough profiles at different bed lengths of 3 cm (1.03 g), 6 cm (2.05 g) and 9 cm (3.1 g) are shown in Figure 3. The decreasing bed length led to a faster breakthrough and saturation process, which resulted in earlier exhaustion of the bed. The increase in the breakthrough time could be attributed to the longer distance and moving time of the mass transfer zone between two ends of the column at a longer bed length (Salman et al., 2011), which was consistent with the calculated lengths of the mass transfer zone in Table 3. On the other hand, the increase in the bed length also led to the increasing mass of ZSM-5 and provided more adsorption sites for MTBE removal. It is noted that, as shown in Table 3, the increase in bed length gave rise to the increase in the total treated MTBE volume and saturation time in Figure 3b; however, the amounts of PVs through the column at saturation time were almost the same for various bed lengths in Figure 3a. This is due to that given the same flow rate and contaminant concentration, the adsorption capacity per unit bed length is constant.

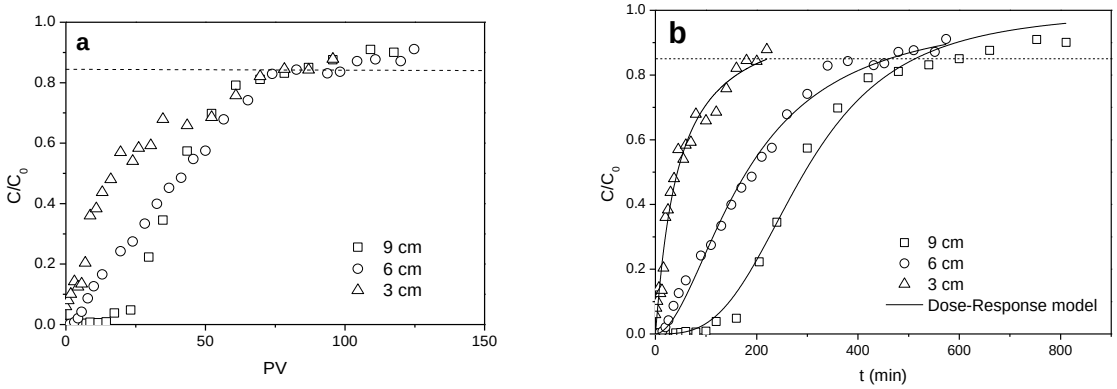

Figure 3 Breakthrough curves at different bed lengths as function of (a) pore volume (PV) and (b) time (t). (flow rate=1 mL·min^{-1}, C_0=300 mg·L^{-1}, ZSM-5 dosage=5%) (adapted from (Zhang et al., 2018a))

In addition, the BDST model was applied to produce the plots of Z versus t in Figure 4 for 5%, 20%, 50%, 60% and 85% saturation of the column with good linearity (R^2>0.9). The

parameters are calculated and listed in Table 4. With the increase of C/C_0 values from 5% (breakthrough point) to 85% (saturation point), the values of N_0 increased from 1787.80 $mg \cdot L^{-1}$ to 4646.93 $mg \cdot L^{-1}$, whereas those of K_{AB} decreased from 1.61×10^{-4} to 5.48×10^{-5} $L \cdot mg^{-1} \cdot min^{-1}$.

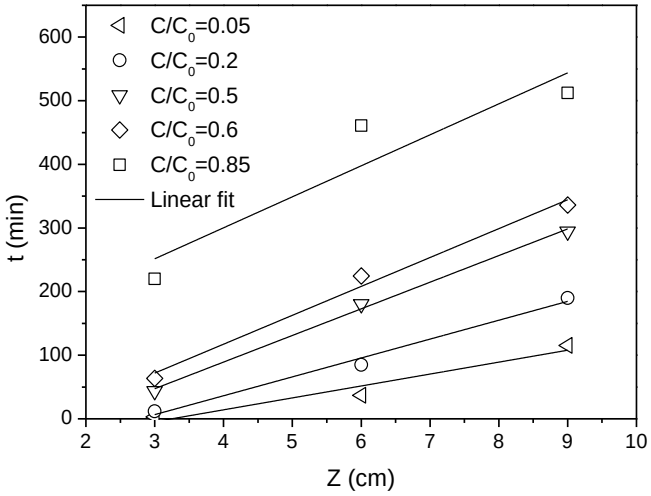

Figure 4 BDST lines at C/C_0 of 0.05, 0.2, 0.5, 0.6, 0.85 with different bed lengths (flow rate=1 $mL \cdot min^{-1}$, C_0=300 $mg \cdot L^{-1}$, ZSM-5 dosage=5%)

Table 4 Calculated parameters of the BDST model for MTBE adsorption on ZSM-5 in the fix-bed column tests

C/C_0	Equations	N_0 ($mg \cdot L^{-1}$)	k_{AB} ($L \cdot mg^{-1} \cdot min^{-1}$)	R^2
0.05	t=18.74Z-60.78	1787.80	1.61×10^{-4}	0.900
0.2	t=29.68Z-82.44	2831.47	5.61×10^{-5}	0.979
0.5	t=41.85Z-78.19	3992.49	0	0.995
0.85	t=48.71Z+105.44	4646.93	5.48×10^{-5}	0.755

The BDST model parameters are of great use for the scale-up of the adsorption process. For example, the groundwater velocities under natural gradient conditions are generally between

1 and 1000 m·year^{-1} (0.002-2 cm·min^{-1}) (Mackay et al., 1985), far lower than the flow rates adopted in this study. According to Equation (12) and (13), the BDST model can be employed to predict the adsorption efficiency and column performance under other operational conditions without further experimental runs (Han et al., 2009a; Vijayaraghavan and Prabu, 2006). Table 5 lists the predicted breakthrough time for a new flow rate (0.01 mL·min^{-1} or 0.003 cm·min^{-1}). Where $t_{c\ is}$ the predicted time and t_e is the observed time in the experiments.

Table 5 Breakthrough time prediction using BDST model at a new flow rate (ZSM-5 percentage=5%)

Operational conditions	C/C_0	New equations	t_c (min)	t_e (min)	RE[a]
Q'=0.5 mL·min^{-1}	0.05	t'=37.48Z-60.78	164.1	167.87	2.25%
Z=6 cm	0.2	t'=59.36Z-82.44	273.72	274.83	0.40%
C_0'=300 mg·L^{-1}	0.5	t'=83.70Z-78.19	424.01	427.09	0.72%
	0.85	t'=97.42Z+105.44	689.96	740.18	6.79%
Q'=0.01 mL·min^{-1}	0.05	t'=1874Z-60.78	11183.22		
Z=6 cm	0.2	t'=2968Z-82.44	17725.56		
C_0=300 mg·L^{-1}	0.5	t'=4185Z-78.19	25031.81		
	0.85	t'=4871Z+105.44	29331.44		

[a] Relative error

It was shown that the values of predicted time at a new flow rate were satisfactory with low relative errors. This indicates that the BDST model parameters in Table 4 can be employed to predict the column performance for the MTBE adsorption of ZSM-5 at different flow rates.

3.3.3 Effect of ZSM-5 dosage

The plots of effluent MTBE concentration versus PV and t at different ZSM-5 dosages are shown in Figure 5a and 5b, respectively.

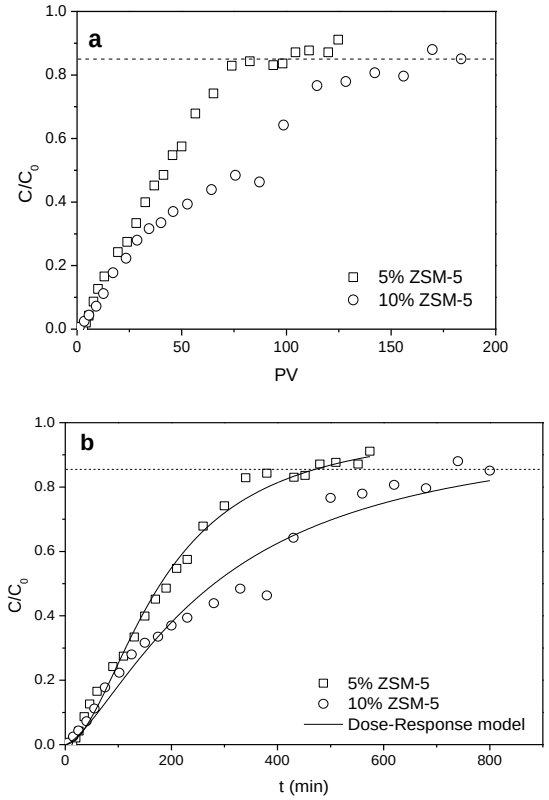

Figure 5 Breakthrough curves in fixed-bed columns with different ZSM-5 percentages as a function of (a) pore volume (PV) and (b) time (t). (C_0=300 mg·L^{-1}, bed length=6 cm, flow rate=1 mL·min^{-1})

The saturation time of the column with a higher ZSM-5 percentage (10%) was significantly longer and its breakthrough curve had a smaller gradient due to more available adsorption sites for MTBE removal in the column. However, the breakthrough time was almost unchanged with different ZSM-5 percentages.

3.3.4 Effect of inlet MTBE concentration

The effect of the influent MTBE concentration at 200, 300 and 400 mg·L^{-1} on the breakthrough profiles was analysed (Figure 6). It was observed that both the breakthrough time and saturation time decreased, and the slope of breakthrough curves between the breakthrough and saturate points, i.e. mass transfer zone (García-Mateos et al., 2015), became slightly steeper with the increase in the influent MTBE concentration. The steeper curve at higher inlet concentrations was an indicator of a smaller effluent volume whereas the extended breakthrough curve at lower inlet MTBE concentrations indicated that more solution was treated (Salman et al., 2011). This is because the higher concentration gradient at higher inlet MTBE concentrations caused a stronger mass transfer driving force (Goel et al., 2005) and faster solute transport in the column, leading to the quicker saturation of the adsorption sites on the ZSM-5 surface. The results in Table 3 show that the highest column adsorption capacity of 27.33 mg·g^{-1} was obtained at the inlet MTBE concentration of 400 mg·L^{-1}. Column tests at a low MTBE level (ug·L^{-1} level) will be explored in future.

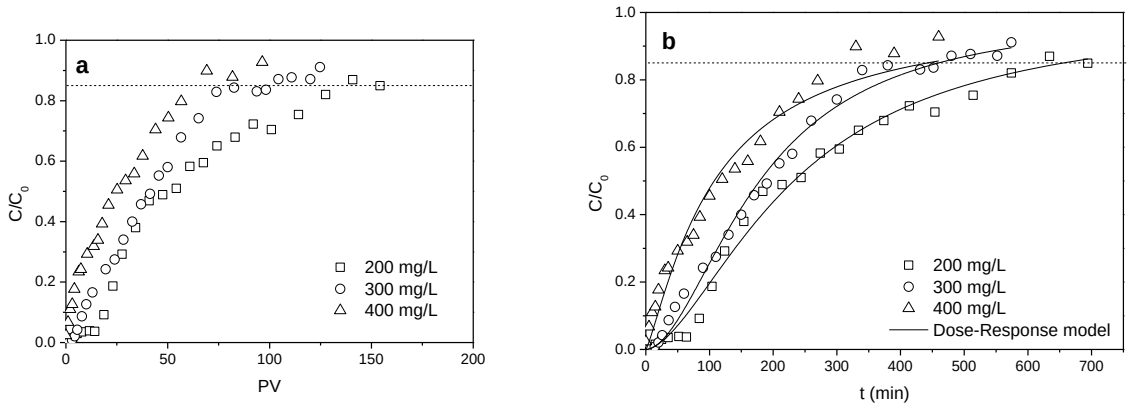

Figure 6 Breakthrough curves at inlet MTBE concentrations of 200, 300 and 400 mg·L^{-1} as function of (a) pore volume (PV) and (b) time (t) (bed length=6 cm, flow rate=1 mL·min^{-1}, ZSM-5=5%)

3.4 Predicted PRB thickness

The flow through thickness of a PRB is a main factor for the PRB design and can be calculated by Equation (13).

$$b = v \times t_w \quad (13)$$

where v is the velocity in the flow direction and t_w is the residence time. The residence time (half-life, t_w) was determined at 99.9% of the respective equilibrium MTBE removal using the best-fitting pseudo-second-order model in our previous study (Zhang et al., 2018) combined with the Solver function in MS Excel (Cai et al., 2018; Gavaskar et al., 2000). The residence time at different initial MTBE concentrations and predicted PRB thicknesses at a nominal groundwater velocity of 0.18 cm·h^{-1} (equivalent to 0.01 mL·min^{-1} pump rate in this study) are listed in Table 6. For example, the predicted PRB flow through thickness was found to be 114.85 cm for 99.9% MTBE removal at an inlet MTBE concentration of 300 mg·L^{-1}.

Table 6 Predicted residence time (h) and PRB thickness (cm) (v=0.18 cm·h^{-1})

Initial MTBE concentration (mg·L^{-1})	100	150	300	600
Residence time (h)	122.62	456.26	638.06	683.11
Thickness (cm)	22.07	82.13	114.85	122.96

There are some limitations of this study, such as (i) the inaccuracy of using batch tests for calculating residence time instead of calculating half-life of MTBE in the column tests; (ii) the use of deionised water without considering the NOM (nature organic matter) and other contaminants in the natural underground water, and (iii) the relatively high flow rate used. More advance column design and selection of a wider range of flow rates will be conducted in future studies to enable more accurate calculations.

Various remediation techniques have been applied to treat MTBE contaminated groundwater, such as classical (Xu et al., 2004) and electrochemical Fenton treatment (Hong et al., 2007), biodegradation by microorganism (Bradley et al., 1999), pump-and-treat, phytoremediation (Hong et al., 2001), PRBs (Obiri-Nyarko et al., 2014), in-situ chemical oxidation (Krembs et al., 2010), etc. The choice of remediation techniques depends on many factors, such as the physiochemical properties of treating agents, site characterization, concentrations of MTBE and other contaminates, and PRB is a promising in-situ groundwater remediation technique due to its low-cost. The PRB treatment of MTBE contaminated groundwater with ZSM-5 as the reactive medium is sustainable due to the adsorption of MTBE onto ZSM-5 without precipitation which may cause clogging and reduce the permeability and removal efficiency of PRBs (Zhou et al., 2014).

3.5 Regeneration study

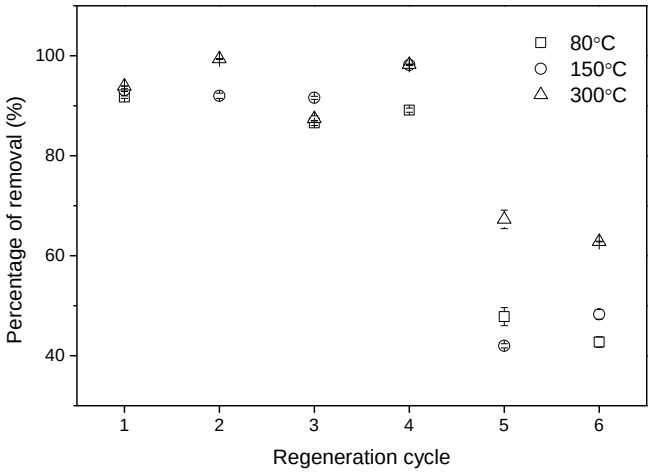

Figure 7 The MTBE removal percentage by ZSM-5 after 6 regeneration cycles

In order to estimate the reusability of ZSM-5, the effect of repeated heat treatment at different temperatures on the MTBE adsorption onto regenerated ZSM-5 was investigated and shown in Figure 7. It was observed that there were no apparent changes in adsorption effects up to

four regeneration cycles at all temperatures and the regeneration at higher temperature slightly increased the removal percentage. The abnormal value at the second cycle at 80 °C was not included due to operating error. However, after 6 regeneration cycles, the removal percentage decreased to ~67% at 300 °C compared with ~47% and ~52% for 80 °C and 150 °C, respectively. Therefore, ZSM-5 displays good regeneration potential compared with modified activated carbon (~18% after 6 cycles) and iron oxide coated zeolites (<6% after 3 cycles) (Ania et al., 2004; Han et al., 2009b). It should be noted that sand or other medium in PRBs should be heated with ZSM-5 in the practical application, and the vaporized MTBE could be collected and treated to avoid secondary pollution.

4. Conclusions

Fixed-bed column tests were combined with breakthrough curve modelling to describe the breakthrough curves and evaluate the adsorption performance under different operational conditions. The regeneration characteristics of ZSM-5 were also discussed. The conclusions are as follows:

(1) The results of both the regeneration tests and fixed-bed column tests show that ZSM-5 is an effective reactive medium in PRBs for MTBE contaminated groundwater remediation.

(2) The Dose-Response model was found to best describe the breakthrough curves compared with the Logit method, Adams-Bohart model, Thomas model and Yoon-Nelson model.

(3) The column adsorption capacity is ~31.85 $mg \cdot g^{-1}$ at a 6 cm bed length, 1 $mL \cdot min^{-1}$ flow rate, 300 $mg \cdot L^{-1}$ initial MTBE concentration and 5% ZSM-5 percentage.

(4) The maximum adsorption capacity increased with the increase of bed length and the decrease of flow rate and MTBE concentration from the Dose-Response model, while the adsorption capacity decreased with a higher ZSM-5 dosage due to the underestimate of

adsorption capacity caused by the fact that the ZSM-5 powder in the column may be more likely to run away with the MTBE flow with a higher ZSM-5 dosage.

(5) The kinetic parameters obtained from the BDST model can be employed to predict the dynamic behaviour of columns at new flow rates.

(6) The adsorption capacity of regenerated ZSM-5 remains satisfactory (>85%) after up to four regeneration cycles at 80, 150 and 300 °C and regeneration at higher temperatures performed slightly better.

Acknowledgements

The first author would like to thank China Scholarship Council (CSC) for providing the PhD studentship, and the third author is grateful to the Killam Trusts of Canada for the Izaak Walton Killam Memorial Postdoctoral Fellowship.

References

Abu-Lail, L., Bergendahl, J.A., Thompson, R.W., 2010. Adsorption of methyl tertiary butyl ether on granular zeolites: Batch and column studies. J. Hazard. Mater. 178, 363–369. https://doi.org/10.1016/j.jhazmat.2010.01.088

Adak, A., Pal, A., 2006. Removal of phenol from aquatic environment by SDS-modified alumina: Batch and fixed bed studies. Sep. Purif. Technol. 50, 256–262. https://doi.org/10.1016/J.SEPPUR.2005.11.033

Al-Tabbaa, A., Liska, M., 2012. Soil mix remediation technology (SMiRT) final technical summary report (confidential).

Anderson, M.A., 2000. Removal of MTBE and other organic contaminants from water by sorption to high silica zeolites. Environ. Sci. Technol. 34, 725–727. https://doi.org/10.1021/es990390t

Ania, C.O., Menéndez, J.A., Parra, J.B., Pis, J.J., 2004. Microwave-induced regeneration of activated carbons polluted with phenol. A comparison with conventional thermal regeneration, in: Carbon. https://doi.org/10.1016/j.carbon.2004.01.010

Ayoob, S., Gupta, A.K., 2007. Sorptive response profile of an adsorbent in the defluoridation of drinking water. Chem. Eng. J. https://doi.org/10.1016/j.cej.2007.02.013

Bohart, G.S., Adams, E.Q., 1920. Some aspects of the behavior of charcoal with respect to chlorine. J. Am. Chem. Soc. 42, 523–544. https://doi.org/10.1021/ja01448a018

Bradley, P.M., Landmeyer, J.E., Chapelle, F.H., 1999. Aerobic mineralization of MTBE and tert-butyl alcohol by stream-bed sediment microorganisms. Environ. Sci. Technol. https://doi.org/10.1021/es990062t

Cai, Q., Turner, B.D., Sheng, D., Sloan, S., 2018. Application of kinetic models to the design of a calcite permeable reactive barrier (PRB) for fluoride remediation. Water Res. https://doi.org/10.1016/j.watres.2017.11.046

Calero, M., Hernáinz, F., Blázquez, G., Tenorio, G., Martín-Lara, M.A., 2009. Study of Cr (III) biosorption in a fixed-bed column. J. Hazard. Mater. 171, 886–893. https://doi.org/10.1016/j.jhazmat.2009.06.082

Cappai, G., De Gioannis, G., Muntoni, A., Spiga, D., Zijlstra, J.J.P., 2012. Combined use of a transformed red mud reactive barrier and electrokinetics for remediation of Cr/As contaminated soil. Chemosphere 86, 400–408. https://doi.org/10.1016/J.CHEMOSPHERE.2011.10.053

Centi, G., Grande, A., Perathoner, S., 2002. Catalytic conversion of MTBE to biodegradable chemicals in contaminated water, in: Catalysis Today. https://doi.org/10.1016/S0920-5861(02)00046-9

Centi, G., Perathoner, S., 2003. Remediation of water contamination using catalytic technologies. Appl. Catal. B Environ. https://doi.org/10.1016/S0926-3373(02)00198-4

Chan, M.S.M., Lynch, R.J., 2003. Photocatalytic degradation of aqueous methyl-tert-butyl-ether (MTBE) in a supported-catalyst reactor. Environ. Chem. Lett. 1, 157–160. https://doi.org/10.1007/s10311-003-0037-4

Cruz Viggi, C., Pagnanelli, F., Cibati, A., Uccelletti, D., Palleschi, C., Toro, L., 2010. Biotreatment and bioassessment of heavy metal removal by sulphate reducing bacteria in fixed bed reactors. Water Res. 44, 151–158. https://doi.org/10.1016/j.watres.2009.09.013

Dorado, A.D., Gamisans, X., Valderrama, C., Solé, M., Lao, C., 2014. Cr(III) removal from aqueous solutions: A straightforward model approaching of the adsorption in a fixed-bed column. J. Environ. Sci. Heal. - Part A Toxic/Hazardous Subst. Environ. Eng. 49, 179–186. https://doi.org/10.1080/10934529.2013.838855

García-Mateos, F.J., Ruiz-Rosas, R., Marqués, M.D., Cotoruelo, L.M., Rodríguez-Mirasol, J., Cordero, T., 2015. Removal of paracetamol on biomass-derived activated carbon:

536 Modeling the fixed bed breakthrough curves using batch adsorption experiments. Chem.
537 Eng. J. 279, 18–30. https://doi.org/10.1016/j.cej.2015.04.144
538 Gavaskar, A., Gupta, N., Sass, B., Janosy, R., Hicks, J., 2000. Design guidance for
539 application of Permeable Reactive Barriers for groundwater remediation.
540 Gavaskar, A.R., 1999. Design and construction techniques for permeable reactive barriers. J.
541 Hazard. Mater. 68, 41–71. https://doi.org/10.1016/S0304-3894(99)00031-X
542 Goel, J., Kadirvelu, K., Rajagopal, C., Kumar Garg, V., 2005. Removal of lead(II) by
543 adsorption using treated granular activated carbon: Batch and column studies. J. Hazard.
544 Mater. 125, 211–220. https://doi.org/10.1016/j.jhazmat.2005.05.032
545 Gouran-Orimi, R., Mirzayi, B., Nematollahzadeh, A., Tardast, A., 2018. Competitive
546 adsorption of nitrate in fixed-bed column packed with bio-inspired polydopamine coated
547 zeolite. J. Environ. Chem. Eng. 6, 2232–2240. https://doi.org/10.1016/j.jece.2018.01.049
548 Han, R., Ding, D., Xu, Y., Zou, W., Wang, Y., Li, Y., Zou, L., 2008. Use of rice husk for the
549 adsorption of congo red from aqueous solution in column mode. Bioresour. Technol. 99,
550 2938–2946. https://doi.org/10.1016/j.biortech.2007.06.027
551 Han, R., Wang, Y., Zhao, X., Wang, Y., Xie, F., Cheng, J., Tang, M., 2009a. Adsorption of
552 methylene blue by phoenix tree leaf powder in a fixed-bed column: Experiments and
553 prediction of breakthrough curves. Desalination 245, 284–297.
554 https://doi.org/10.1016/j.desal.2008.07.013
555 Han, R., Zou, L., Zhao, X., Xu, Y., Xu, F., Li, Y., Wang, Y., 2009b. Characterization and
556 properties of iron oxide-coated zeolite as adsorbent for removal of copper(II) from
557 solution in fixed bed column. Chem. Eng. J. 149, 123–131.
558 https://doi.org/10.1016/j.cej.2008.10.015
559 Hong, M.S., Farmayan, W.F., Dortch, I.J., Chiang, C.Y., McMillan, S.K., Schnoor, J.L., 2001.
560 Phytoremediation of MTBE from a groundwater plume. Environ. Sci. Technol.

561 https://doi.org/10.1021/es001911b
562 Hong, S., Zhang, H., Duttweiler, C.M., Lemley, A.T., 2007. Degradation of methyl tertiary-
563 butyl ether (MTBE) by anodic Fenton treatment. J. Hazard. Mater.
564 https://doi.org/10.1016/j.jhazmat.2006.12.030
565 Hou, D., Al-Tabbaa, A., Luo, J., 2014. Assessing effects of site characteristics on remediation
566 secondary life cycle impact with a generalised framework. J. Environ. Plan. Manag. 57,
567 1083–1100. https://doi.org/10.1080/09640568.2013.863754
568 Hutchins, R., 1973. New method simplifies design of activated-carbon systems. Chem. Eng.
569 80, 133–138.
570 Jha, B., Singh, D.N., 2016. Fly ash zeolites, Advanced Structured Materials. Springer
571 Singapore, Singapore. https://doi.org/10.1007/978-981-10-1404-8
572 Katsou, E., Malamis, S., Tzanoudaki, M., Haralambous, K.J., Loizidou, M., 2011.
573 Regeneration of natural zeolite polluted by lead and zinc in wastewater treatment
574 systems. J. Hazard. Mater. 189, 773–786. https://doi.org/10.1016/j.jhazmat.2010.12.061
575 Krembs, F.J., Siegrist, R.L., Crimi, M.L., Furrer, R.F., Petri, B.G., 2010. ISCO for
576 groundwater remediation: Analysis of field applications and performance. Gr. Water
577 Monit. Remediat. https://doi.org/10.1111/j.1745-6592.2010.01312.x
578 Levchuk, I., Bhatnagar, A., Sillanpää, M., 2014. Overview of technologies for removal of
579 methyl tert-butyl ether (MTBE) from water. Sci. Total Environ.
580 https://doi.org/10.1016/j.scitotenv.2014.01.037
581 Lindsey, B.D., Ayotte, J.D., Jurgens, B.C., Desimone, L.A., 2017. Using groundwater age
582 distributions to understand changes in methyl tert-butyl ether (MtBE) concentrations in
583 ambient groundwater, northeastern United States. Sci. Total Environ. 579, 579–587.
584 https://doi.org/10.1016/j.scitotenv.2016.11.058
585 Mackay, D.M., Roberts, P. V., Cherry, J.A., 1985. Transport of organic contaminants in

groundwater. Environ. Sci. Technol. 19, 384–392. https://doi.org/10.1021/es00135a001

Mancini, E.R., Steen, A., Rausina, G.A., Wong, D.C.L., Arnold, W.R., Gostomski, F.E., Davies, T., Hockett, J.R., Stubblefield, W.A., Drottar, K.R., Springer, T.A., Errico, P., 2002. MTBE ambient water quality criteria development: A public/private partnership. Environ. Sci. Technol. 36, 125–129. https://doi.org/10.1021/es002059b

Martucci, A., Braschi, I., Bisio, C., Sarti, E., Rodeghero, E., Bagatin, R., Pasti, L., 2015. Influence of water on the retention of methyl tertiary-butyl ether by high silica ZSM-5 and Y zeolites: a multidisciplinary study on the adsorption from liquid and gas phase. RSC Adv. 5, 86997–87006. https://doi.org/10.1039/C5RA15201A

Masad, E., Taha, R., Ho, C., Papagiannakis, T., 1996. Engineering properties of tire/soil mixtures as a lightweight fill material. Geotech. Test. Journal, 19, 297–304. https://doi.org/10.1520/GTJ10355J

Mohebali, S., 2013. Degradation of methyl t-butyl ether (MTBE) by photochemical process in nanocrystalline TiO2 slurry: Mechanism, by-products and carbonate ion effect. J. Environ. Chem. Eng. 1, 1070–1078. https://doi.org/10.1016/j.jece.2013.08.022

Obiri-Nyarko, F., Grajales-Mesa, S.J., Malina, G., 2014. An overview of permeable reactive barriers for in situ sustainable groundwater remediation. Chemosphere. https://doi.org/10.1016/j.chemosphere.2014.03.112

Oulman, C., 1980. The logistic curve as a model for carbon bed design. J. AWWA 72, 50–53.

Ozdemir, O., Turan, M., Turan, A.Z., Faki, A., Engin, A.B., 2009. Feasibility analysis of color removal from textile dyeing wastewater in a fixed-bed column system by surfactant-modified zeolite (SMZ). J. Hazard. Mater. 166, 647–654. https://doi.org/10.1016/j.jhazmat.2008.11.123

Pascoe, W.E., 1992. Catalysis of organic reactions. Marcel Dekker, New York.

Reuter, J.E., Allen, B.C., Richards, R.C., Pankow, J.F., Goldman, C.R., Roger L. Schol, A.,

611 Seyfried, J.S., 1998. Concentrations, sources, and fate of the gasoline oxygenate Methyl
612 tert-Butyl Ether (MTBE) in a multiple-use lake. Environ. Sci. Technol. 32, 3666–3672.
613 https://doi.org/10.1021/ES9805223
614 Sağ, Y., Aktay, Y., 2001. Application of equilibrium and mass transfer models to dynamic
615 removal of Cr(VI) ions by Chitin in packed column reactor. Process Biochem. 36, 1187–
616 1197. https://doi.org/10.1016/S0032-9592(01)00150-9
617 Salman, J., Njoku, V., Hameed, B., 2011. Batch and fixed-bed adsorption of 2, 4-
618 dichlorophenoxyacetic acid onto oil palm frond activated carbon. Chem. Eng. J. 174,
619 33–40.
620 Shah, I.K., Pre, P., Alappat, B.J., 2014. Effect of thermal regeneration of spent activated
621 carbon on volatile organic compound adsorption performances. J. Taiwan Inst. Chem.
622 Eng. 45, 1733–1738. https://doi.org/10.1016/J.JTICE.2014.01.006
623 Thomas, H., 1944. Heterogeneous ion exchange in a flowing system. J. Am. Chem. Soc. 66,
624 1664–1666.
625 Thomas, H.C., 1948. Chromatography: A problem in kinetics. Ann. N. Y. Acad. Sci. 49,
626 161–182. https://doi.org/10.1111/j.1749-6632.1948.tb35248.x
627 Vijayaraghavan, K., Prabu, D., 2006. Potential of Sargassum wightii biomass for copper(II)
628 removal from aqueous solutions: Application of different mathematical models to batch
629 and continuous biosorption data. J. Hazard. Mater. 137, 558–564.
630 https://doi.org/10.1016/j.jhazmat.2006.02.030
631 Wang, S., Zhu, Z.H., 2006. Characterisation and environmental application of an Australian
632 natural zeolite for basic dye removal from aqueous solution. J. Hazard. Mater. 136, 946–
633 952. https://doi.org/10.1016/j.jhazmat.2006.01.038
634 Wei, Y.X., Ye, Z.F., Wang, Y.L., Ma, M.G., Li, Y.F., 2011. Enhanced ammonia nitrogen
635 removal using consistent ammonium exchange of modified zeolite and biological

636 regeneration in a sequencing batch reactor process. Environ. Technol. 32, 1337–1343.
637 https://doi.org/10.1080/09593330.2010.536784
638 Xin, S., Zeng, Z., Zhou, X., Luo, W., Shi, X., Wang, Q., Deng, H., Du, Y., 2017. Recyclable
639 Saccharomyces cerevisiae loaded nanofibrous mats with sandwich structure constructing
640 via bio-electrospraying for heavy metal removal. J. Hazard. Mater. 324, 365–372.
641 https://doi.org/10.1016/j.jhazmat.2016.10.070
642 Xu, X.R., Zhao, Z.Y., Li, X.Y., Gu, J.D., 2004. Chemical oxidative degradation of methyl
643 tert-butyl ether in aqueous solution by Fenton's reagent. Chemosphere.
644 https://doi.org/10.1016/j.chemosphere.2003.11.017
645 Yan, G., Viraraghavan, T., Chen, M., 2001. A new model for heavy metal removal in a
646 biosorption column. Adsorpt. Sci. Technol. 19, 25–43.
647 https://doi.org/10.1260/0263617011493953
648 Yoon, Y.H., 1984. Application of gas adsorption kinetics. A Theor. Model Respir. Cart. Serv.
649 life 45, 509–516.
650 Zhang, Y., Jin, F., Lynch, R., Al-Tabbaa, A., 2018a. Breakthrough curve modelling of ZSM-
651 5 zeolite packed fixed-bed columns for the removal of MTBE, in: The 8th International
652 Congress on Environmental Geotechnics (Forthcoming).
653 Zhang, Y., Jin, F., Shen, Z., Lynch, R., Al-Tabbaa, A., 2018b. Kinetic and equilibrium
654 modelling of MTBE (methyl tert-butyl ether) adsorption on ZSM-5 zeolite: Batch and
655 column studies. J. Hazard. Mater. 347, 461–469.
656 https://doi.org/10.1016/J.JHAZMAT.2018.01.007
657 Zhou, D., Li, Y., Zhang, Y., Zhang, C., Li, X., Chen, Z., Huang, J., Li, X., Flores, G., Kamon,
658 M., 2014. Column test-based optimization of the permeable reactive barrier (PRB)
659 technique for remediating groundwater contaminated by landfill leachates. J. Contam.
660 Hydrol. https://doi.org/10.1016/j.jconhyd.2014.09.003

Adsorption of Methyl tert-butyl ether (MTBE) onto ZSM-5 zeolite: Fixed-bed column tests, breakthrough curve modelling and regeneration

Yunhui Zhang[a]; Fei Jin[b]; Zhengtao Shen[c]; Fei Wang[d]; Rod Lynch[a]; Abir Al-Tabbaa[a]*

[a]Department of Engineering, University of Cambridge, Cambridge, CB2 1PZ, United Kingdom

[b]School of Engineering, University of Glasgow, Glasgow, G12 8QQ, United Kingdom

[c]Department of Earth and Atmospheric Sciences, University of Alberta, Edmonton T6G 2E3, Canada

[d]Institute of Geotechnical Engineering, School of Transportation, Southeast University, Nanjing, 210096, China

AUTHOR INFORMATION

***Corresponding Author**

Tel: +44- (0) 7821464199

E-mail address: yz485@cam.ac.uk.

Abstract

ZSM-5, as a hydrophobic zeolite, has a good adsorption capacity for methyl tert-butyl ether (MTBE) in batch adsorption studies. This study explores the applicability of ZSM-5 as a reactive material in permeable reactive barriers (PRBs) to decontaminate the MTBE-containing groundwater. A series of laboratory scale fixed-bed column tests were carried out to determine the breakthrough curves and evaluate the adsorption performance of ZSM-5 towards MTBE under different operational conditions, including bed length, flow rate, initial MTBE concentration and ZSM-5 dosage, and regeneration tests were carried out at 80, 150 and 300 °C for 24 h. Dose-Response model was found to best describe the breakthrough curves. MTBE was effectively removed by the fixed-bed column packed with a ZSM-5/sand mixture with an adsorption capacity of 31.85 $mg \cdot g^{-1}$ at 6 cm bed length, 1 $mL \cdot min^{-1}$ flow rate, 300 $mg \cdot L^{-1}$ initial MTBE concentration and 5% ZSM-5 dosage. The maximum adsorption capacity increased with the increase of bed length and the decrease of flow rate and MTBE concentration. The estimated kinetic parameters can be used to predict the dynamic behaviour of column systems. In addition, regeneration study shows that the adsorption capacity of ZSM-5 remains satisfactory (>85%) after up to four regeneration cycles.

Key words: MTBE, ZSM-5 zeolite, Fixed-bed column tests, Permeable reactive barriers, Regeneration

1. Introduction

Gasoline spills from the accidental leakage of storage tanks, transfer pipes and boats are typical pollution sources of soil, groundwater, surface water and the marine environment (Reuter et al., 1998). Methyl tert-butyl ether (MTBE) was an extensively used gasoline additive for fuel oxygenation. In spite of the bans in some countries, it is still the second most common volatile organic compound in shallow groundwater (Levchuk et al., 2014). Due to its genotoxicity, its hazard of causing skin and eye irritation and its unpleasant odour (Mancini et al., 2002), the existence of MTBE in aquatic environments has raised considerable public concerns.

Permeable reactive barriers (PRBs) is an effective in-situ technology for aquifer and groundwater remediation (Hou et al., 2014). Due to the rapid migration (Levchuk et al., 2014) and limited natural biodegradation potential of MTBE (Lindsey et al., 2017; Mohebali, 2013), using PRBs to mitigate/eliminate MTBE contamination holds much promise. As the key component of PRBs, the reactive medium is selected primarily depending on the nature of target contaminants and the hydro-geological conditions of field sites. ZSM-5 as a reactive medium in the PRBs can act as adsorbents due to its high adsorption capacity (Abu-Lail et al., 2010; Martucci et al., 2015; Zhang et al., 2018b) and hydrogen form of ZSM-5 (HZSM-5) may also catalyse the hydrolysis of MTBE to *t*-butyl alcohol (TBA) and methanol which are more biodegradable (Centi et al., 2002; Knappe and Campos, 2005). These products can also be adsorbed onto ZSM-5 and be released slowly with time which favours their biodegradation by microorganisms growing on the barrier (Centi and Perathoner, 2003). The PRBs design requires a kinetic characterisation using fixed-bed columns as a simulation of real PRBs to evaluate the dynamic removal of contaminants for the practical application (Cruz Viggi et al., 2010; Gavaskar, 1999). Various theoretical models, such as Logit, Adams-

Bohart, Thomas, Yoon and Nelson, Dose and Response, and bed length/service time (BDST) models, have been developed to fit the experimental data and obtain the breakthrough curves and column kinetic parameters. These parameters can be employed to predict the adsorption performance under new operational conditions and further facilitate the full-scale design of fixed-bed column systems, e.g., PRBs.

To date, fixed-bed column tests have been widely applied to simulate PRBs towards various contaminants, such as heavy metals and dyes (Calero et al., 2009; Han et al., 2008), with different adsorbents such as activated carbon and zeolites (García-Mateos et al., 2015; Ozdemir et al., 2009) etc. Nevertheless, to our best knowledge, limited studies exist on fixed-bed column tests of using ZSM-5 for MTBE removal, especially regarding the influence of operational conditions, such as the bed length, flow rate, inlet adsorbate concentrations and the percentage of the adsorbent on the adsorption behaviour. Abu-Lail et al. (2010) studied the removal of MTBE with three adsorbents including granular ZSM-5 in large and small diameter fixed-bed columns, and evaluated the influence of bed length on the breakthrough curves with the BDST model. It was shown that the granular ZSM-5 with a shorter bed length reached the breakthrough point earlier due to the less mass of adsorbents in the column. However, besides the bed length, other variables, such as flow rate, the MTBE concentration and ZSM-5 dosage, also need to be considered in practical groundwater contamination applications due to the fact that the groundwater flow rate and MTBE concentrations vary in different regions. Therefore, this study discussed the influence of several operational parameters (bed length, flow rate, initial MTBE concentration and ZSM-5 percentage) in fixed-bed column tests. The parameters obtained from modelling are crucial for PRB design and can be used to guide the application of ZSM-5 as a reactive medium in the PRBs for the MTBE-contaminated groundwater remediation.

Reusability is considered as a key criterion to judge the feasibility of an adsorbent in practical applications (Xin et al., 2017). The exhausted adsorbents are generally considered as hazardous wastes and need to be incinerated, leading to secondary pollution, such as thermal pollution and potential desorption of adsorbate in the atmosphere (Shah et al., 2014). The regeneration of spent adsorbents can recover material resources, minimize the demands of virgin adsorbents and avoid the generation of hazardous waste. Zeolites, including ZSM-5, demonstrate good stability under a wide range of environmental conditions, such as acidic (Pascoe, 1992) and high temperature environments (Anderson, 2000). They can be regenerated by heat treatment, chemical treatment, such as Fenton oxidation (Wang and Zhu, 2006) and KCl (Katsou et al., 2011), and biological regeneration (Wei et al., 2011). However, chemical or biological methods may lead to the generation of hazardous residues. Although HZSM-5 may adsorb and catalyse the hydrolysis of MTBE, and then release the adsorbed reaction products (TBA and methanol) to achieve self-regeneration, this process takes a long time (Centi and Perathoner, 2003) and our previous study showed that the desorption was negligible after 3 days in batch tests (Zhang et al., 2018b). Further studies will investigate the long term behaviour. Thermal regeneration is effective and time-saving for adsorbents used for volatile and semi-volatile organic compounds, including MTBE, due to its high vapour pressure under normal temperatures and low boiling points. In this study, in order to avoid excessive consumption of materials and secondary pollution, repeated thermal regeneration was used for the regeneration of ZSM-5 to evaluate the stability of ZSM-5 after several adsorption-desorption cycles.

This study aims to (1) analyse the effects of various operational conditions (flow rate, bed length, initial MTBE concentration and ZSM-5 percentage) in fixed-bed column tests on the

MTBE adsorption onto ZSM-5; (2) find the most suitable model to describe the breakthrough curve and obtain column parameters; (3) predict adsorption performance at a new flow rate without further experimental runs with the BDST model and (4) examine the recyclability of ZSM-5 with repeated thermal regeneration tests.

2. Materials and methods

2.1 Materials

MTBE was purchased from Fisher Scientific, and hydrogen form of ZSM-5 powder was obtained from Acros Organics. ZSM-5 used in this study has a large surface area of 400 $m^2 \cdot g^{-1}$ and a high SiO_2/Al_2O_3 ratio of 469. Two pore systems, i.e. zig-zag channels and straight channels, exist in the structure of ZSM-5 with pore sizes of 5.3×5.6 Å and 5.1×5.5 Å, respectively. The detailed physicochemical properties and framework structure of ZSM-5 can be found in (Zhang et al., 2018b).

2.2 Fixed-bed column tests

A series of fixed-bed column tests were conducted in a Pyrex glass column (2 cm inner diameter and 10 cm high) for the simulation of ZSM-5 containing PRBs for MTBE adsorption. There is a layer of glass beads and a stainless steel mesh filter attached to each end of the column to ensure the uniform flow of the solution. The schematic of the fixed-bed column set-up is shown in Figure 1.

Figure 1 The schematic of the fixed-bed column set-up in this study

ZSM-5 was mixed with sand to increase the permeability due to the fine texture of ZSM-5 (Cappai et al., 2012). Columns were filled with a mixture of ZSM-5 (5% or 10% in w/w of sand) and sand to produce different bed lengths (3, 6 and 9 cm). The initial water content of the specimen was designated as 10% in w/w (of sand) and the bulk density was about 2 $g \cdot cm^{-3}$. The values of hydraulic conductivity of the mixture in the column were measured as 6.32 $\times 10^{-6}$ $m \cdot s^{-1}$ (5% ZSM-5 and sand) and 1.21 $\times 10^{-6}$ $m \cdot s^{-1}$ (10% ZSM-5 and sand). It was assumed that the specific gravity values of sand and ZSM-5 were 2.65 and 2 respectively in this study (Jha and Singh, 2016; Masad et al., 1996). It is noted that the seepage velocity differs at different regions and different depths (Gavaskar et al., 2000). Therefore in this study, pump rate (i.e., seepage rate) was selected based on a previous land remediation project with sandy soils in the ground (Al-Tabbaa and Liska, 2012). The solutions with different MTBE concentrations (200, 300 and 400 $mg \cdot L^{-1}$) were pumped upward at different flow rates of 0.5 $mL \cdot min^{-1}$ (seepage velocity: 0.011 $cm \cdot s^{-1}$), 1 $mL \cdot min^{-1}$ (seepage velocity: 0.022 $cm \cdot s^{-1}$) and 2 $mL \cdot min^{-1}$ (seepage velocity: 0.044 $cm \cdot s^{-1}$) controlled by a peristaltic pump. Flow rates and MTBE concentrations in this study were higher than the actual conditions in

most regions to save the operational time in the lab. Also, the PRBs were generally installed near pollution sources with a high MTBE concentration.

The detailed operation variables are listed in Table 1. Where m_{ZSM-5} is the mass of ZSM-5 in the column (g). The effect of flow rate was studied by tests C, F0.5 and F2; the effect of bed length was examined by tests C, B3 and B9; tests C and Z10 were conducted to discuss the effect of ZSM-5 dosage and tests C, M200 and M400 ascertained the effect of initial MTBE concentration. The effluents at the outlet were collected at set intervals and the MTBE concentration was measured. The saturation time (t_s) was established when the effluent MTBE concentration exceeded 85% of inlet concentration. The breakthrough time (t_b) (Goel et al., 2005) is established when the effluent MTBE concentration reaches 5% of the inlet concentration (C/C_0=0.05) (García-Mateos et al., 2015).

Table 1 Operational variables for fixed-bed column tests

Test No.	Influencing factors	Flow rate ($mL \cdot min^{-1}$)	Bed length (cm)	m_{ZSM-5} (g)	ZSM-5 (%)	C_0 (MTBE) ($mg \cdot L^{-1}$)	Porosity
F0.5	Flow rate	0.5	6	2.05	5	300	0.25
C	Flow rate	1	6	2.05	5	300	0.24
F2	Flow rate	2	6	2.05	5	300	0.24
B3	Bed length	1	3	1.03	5	300	0.24
C	Bed length	1	6	2.05	5	300	0.24
B9	Bed length	1	9	3.08	5	300	0.24
C	ZSM-5 dosage	1	6	2.05	5	300	0.24
Z10	ZSM-5 dosage	1	6	4.50	10	300	0.23

M200	MTBE concentration	1	6	2.07	5	200	0.24
C	MTBE concentration	1	6	2.05	5	300	0.24
M400	MTBE concentration	1	6	2.03	5	400	0.25

168

169 2.3 Regeneration cycles

170 The thermal regeneration tests were conducted to examine the recyclability of ZSM-5 at
171 different temperatures based on batch adsorption tests. After MTBE adsorption in aqueous
172 solution with ZSM-5, the saturated ZSM-5 was heated at 80, 150 or 300 °C for 24 h in a
173 muffle furnace (Carbolite CWF 1200, UK), and then 0.1 g of regenerated ZSM-5 was added
174 to 20 mL 300 $mg \cdot L^{-1}$ of MTBE solution for adsorption for 24h. After each regeneration cycle,
175 the MTBE removal percentage was determined and this process was repeated up to 6 times.

176

177 2.4 Analytical methods

178 MTBE concentration was analysed by an ambient headspace technique as described in our
179 previous studies (Chan and Lynch, 2003; Zhang et al., 2018b) using a gas chromatograph
180 (Agilent 6850 Series) with a flame ionisation detector (GC-FID). Each headspace sample was
181 measured in triplicate. Data fitting and modelling was performed by OriginPro 8.5 software.
182 The values of Akaike information criterion (AIC) and correlation coefficient (R^2) were used
183 to compare different models. The lower AIC and higher R^2 values indicate a more suitable
184 model.

185

186 2.5 Mathematical models for breakthrough curves

The operational parameters, such as the breakthrough time, saturation time, the shape of breakthrough curves and the column adsorption capacity, play important roles in the evaluation of the operational and adsorption performance of columns. They can be obtained from a plot of C/C_0 against time (t) using the non-linear regression method. Several mathematical models, such as Adams-Bohart model, the Logit method, Thomas model, Yoon-Nelson model and Dose-Response model, have been developed and widely applied to fit the experimental data of column tests to predict the concentration-time profiles and breakthrough curves. Therefore, these models were used in this study to find the most suitable model to describe the breakthrough curve and obtain maximum column capacity. This will help avoid unnecessary investment and high operational costs in the design and operation of a full-scale column caused by possible underutilized or oversaturated columns.

2.5.1 Adams-Bohart model

The Adams-Bohart model (Bohart and Adams, 1920) was developed based on the assumption that adsorption rate is proportional to the adsorbent's residual capacity and the adsorbate's concentration (Goel et al., 2005). It is generally used to describe the initial portion ($C/C_0<0.15$) of the breakthrough curve and has been extensively applied in other various systems (Calero et al., 2009; Sağ and Aktay, 2001). The expression is given as follows

$$\frac{C}{C_0} = \frac{e^{k_{AB}C_0 t}}{e^{(k_{AB}N_0 Z/v)} - 1 + e^{k_{AB}C_0 t}} \quad (1)$$

where k_{AB} is the rate constant ($L \cdot mg^{-1} \cdot min^{-1}$) and N_0 is the volumetric adsorption capacity ($mg \cdot L^{-1}$).

2.5.2 Bed depth/service time (BDST) model

BDST model (Oulman, 1980) is rearranged from the Adams-Bohart model by Hutchins (Hutchins, 1973) to produce a linear relationship between the bed length (Z, cm) and service time (t, min). It is based on the assumption that the moving speed of the adsorption zone in the column is constant, and can be described as follows:

$$t = \frac{N_0}{C_0 v} Z - \frac{1}{C_0 k_{AB}} \ln\left(\frac{C_0}{C} - 1\right) \quad (2)$$

$$a = \frac{N_0}{C_0 v} \quad (3)$$

$$b = \frac{1}{C_0 k_{AB}} \ln\left(\frac{C_0}{C} - 1\right) \quad (4)$$

The values of N_0 and k_{AB} can be obtained from a plot of Z against t. The advantage of the BDST model is that only three column tests are required to collect the experimental data (Adak and Pal, 2006; Hutchins, 1973).

For a new operational condition, such as a new linear flow rate (v'), the new slope (a') and intercept (b') can be calculated directly by Equation (5) and (6), respectively.

$$a' = a\frac{v}{v'} \quad (5)$$

$$b' = b \quad (6)$$

2.5.3 Logit method

BDST model may cause errors if the service time at which the effluent exceeds the breakthrough criteria was selected. Therefore, Logit method was established to provide a rational basis for the fitting to the data and the reduction of errors (Oulman, 1980).

The equation of the Logit method (Oulman, 1980) can be written as

$$ln\left(\frac{\frac{C}{C_0}}{1-\frac{C}{C_0}}\right) = KC_0 t - \frac{KNZ}{v} \quad (7)$$

To apply it to describe the breakthrough curve, Equation (7) is rearranged as

$$\frac{C}{C_0} = \frac{e^{(KC_0 t - KNZ/v)}}{1+e^{(KC_0 t - KNZ/v)}} \quad (8)$$

where v is the linear flow rate ($cm \cdot min^{-1}$), C is the solute concentration ($mg \cdot L^{-1}$), C_0 is the inlet MTBE concentration ($mg \cdot L^{-1}$), K is the adsorption rate coefficient ($L \cdot mg^{-1} \cdot min^{-1}$) and N is the adsorption capacity coefficient ($mg \cdot L^{-1}$).

2.5.4 Thomas model

Thomas model (Equation (9)) based on the mass-transfer theory and was used to calculate the maximum adsorption capacity (q_0, $mg \cdot g^{-1}$) and the Thomas adsorption rate constant (K_{Th}, $L \cdot mg^{-1} \cdot min^{-1}$) using experimental data from fixed-bed column tests (Thomas, 1944, 1948).

$$\frac{C}{C_0} = \frac{1}{1+e^{\frac{k_{Th}}{Q}(q_0 m - C_0 V)}} \quad (9)$$

where V is the effluent volume (L), m is the mass of adsorbent (g), and Q is the flow rate of the influent ($L \cdot min^{-1}$).

2.5.5 Yoon and Nelson model

The wide use of Yoon and Nelson model (Yoon, 1984) in single adsorbate systems is attributed to its simplicity since no detailed data is needed regarding the properties of adsorbate, adsorbent and the column. The equation is given by:

$$\frac{C}{C_0} = \frac{1}{1+e^{k_{YN}(\tau - t)}} \quad (10)$$

where τ is the time required for 50% adsorbate breakthrough (min) and k_{YN} is the rate constant (min^{-1}). This model assumes that the declining rate in the probability of adsorption is proportional to that of both adsorbate adsorption and adsorbate breakthrough on the adsorbent (Ayoob and Gupta, 2007).

2.5.6 Dose-Response model

Dose-Response model (Yan et al., 2001) is an empirical model and has been widely used to describe the column kinetics and behaviour, especially heavy metal removal (Dorado et al., 2014). The general equation is as follows:

$$\frac{C}{C_0} = 1 - \frac{1}{1+(\frac{C_0 V}{q_0 m})^a} \quad (11)$$

$$b = V_{(50\%)} = \frac{q_0 m}{C_0} \quad (12)$$

where a is the constant, b is equal to $V_{(50\%)}$, the concentration when 50% of the maximum response occurs (L).

3. Results and discussion

3.1 Breakthrough curve modelling

The concentration-time profiles were obtained after a series of fixed-bed column experiments. Five models were applied to fit the experimental data to describe the fixed-bed column behaviour. The empirical Dose-Response model best described the experimental data in different column conditions (R^2>0.95 with the lowest AIC value), suggesting its suitability to be used for the design and scale-up purpose. This model was also shown to reduce the errors of two conventional mathematical models, i.e. Thomas model and Adams-Bohart model, for the biosorption of heavy metals in a column (Yan et al., 2001). The fitting results of the Dose-Response model are shown in Table 2 and those of other models are shown in Table S1 and Figure S1-S4 in the Appendix.

From Table 2, the values of q_0 increased with the increase of bed length and the decrease of flow rate, ZSM-5 dosage and initial MTBE concentration. The adsorption capacity (q_0) was calculated as 26.32 $mg \cdot g^{-1}$ at 6 cm bed length, 1 $mL \cdot min^{-1}$ flow rate, 300 $mg \cdot L^{-1}$ initial MTBE concentration and 5% ZSM-5 dosage (Test No. C).

Table 2 Dose-Response model parameters for the MTBE adsorption on ZSM-5 under different operational conditions

Variables	Test No.	a	b (mL)	q_0 ($mg \cdot g^{-1}$)	R^2
Flow rate	C	1.84	179.88	26.32	0.993
	F0.5	3.14	213.16	31.19	0.997
	F2	0.95	90.99	13.32	0.959
Bed length	C	1.84	179.88	26.32	0.993
	B3	1.06	43.46	12.66	0.997

	B9	3.14	294.63	28.70	0.991
ZSM-5 percentage	C	1.84	179.88	26.32	0.993
	Z10	1.45	280.78	18.72	0.971
Initial MTBE	C	1.84	179.88	26.32	0.993
concentration	M200	1.67	232.38	22.45	0.989
	M400	1.23	107.34	21.15	0.969

277

278 3.2 Column parameters calculation

279 The column adsorption capacity of the adsorbent is a critical indicator of column
280 performance and could be calculated from the breakthrough curve. Considering the best
281 fitting results of the Dose-Response model in Session 3.1, all the breakthrough parameters
282 under certain operational conditions were calculated based on the Dose-Response model
283 fitting and are listed in Table 3. Where MTZ is the length of the mass transfer zone (cm),
284 m_{adsorb} is the adsorbed amount of MTBE (mg), m_{total} is the total amount of MTBE through the
285 column (mg), q_e is the equilibrium MTBE uptake, also called column maximum separation
286 capacity ($mg \cdot g^{-1}$) (Gouran-Orimi et al., 2018), C_e is the equilibrium MTBE concentration
287 ($mg \cdot L^{-1}$), and R is the total MTBE removal percentage (%).

288

289 It is obvious that both the breakthrough time and saturation time increased with the
290 decreasing flow rate and initial MTBE concentration. The same trend was shown when the
291 bed length or ZSM-5 dosage were increased. The maximum column separation capacity is
292 31.85 $mg \cdot g^{-1}$ at 6 cm bed length, 1 $mL \cdot min^{-1}$ flow rate, 300 $mg \cdot L^{-1}$ initial MTBE
293 concentration and 5% ZSM-5 dosage (Test No. C) in this study. In comparison, the maximum
294 adsorption capacity in batch adsorption tests were calculated as 53.55 $mg \cdot g^{-1}$ in our previous
295 study (Zhang et al., 2018b), which almost doubled that in fixed-bed column tests (31.85

296 mg·g^{-1}). This is mainly due to the insufficient contact time between ZSM-5 and MTBE in
297 columns (461 min and 24 h for column tests and batch tests, respectively). It should be noted
298 that both the adsorption capacity (q_0 in Table 2) and the maximum column separation
299 capacity (q_e in Table 3) decreased with a higher ZSM-5 percentage in spite of a higher
300 adsorbed amount of MTBE (m_{adsorb} in Table 3). This may be explained by the phenomenon
301 that ZSM-5 was easier to run away with the MTBE flow with a higher ZSM-5 dosage,
302 leading to an underestimate of the adsorption capacity, which is a limitation of this study.
303
304 Table 3 Parameters of breakthrough curves for MTBE adsorption on ZSM-5 in fixed-bed
305 columns under different operational conditions

Test No.	C	F0.5	F2	B3	B9	Z10	M200	M400
t_b (min)	36.77	167.87	2.08	2.86	115.28	36.84	40.29	10.13
t_s (min)	460.81	740.18	260.00	220.00	512.25	919.75	655.79	442.04
$MTZ = \frac{Z(t_s - t_b)}{t_s}$ (cm)	5.52	4.64	5.95	2.96	6.97	5.76	5.63	5.86
$m_{adsorb} = \frac{Q}{1000}\int_{t=0}^{t=t_{total}}(C_0 - C)dt$ (mg)	65.30	67.42	52.99	23.01	93.23	114.99	52.77	66.52
$m_{total} = \frac{C_0 Q t_{total}}{1000}$ (mg)	138.24	111.03	156.00	66.00	153.68	275.93	131.16	176.82
$q_e = \frac{m_{adsorb}}{m_{zsm-5}}$ (mg·g^{-1})	31.85	32.89	25.85	22.34	30.27	25.55	25.49	32.77
$C_e = \frac{1000(m_{total} - m_{adsorb})}{Q t_{total}}$ (mg·L^{-1})	158.29	117.82	198.10	195.42	118.00	174.98	119.53	249.52
$R = \frac{100 m_{adsorb}}{m_{total}}$ (%)	47.24	60.73	33.97	34.86	60.67	41.67	40.23	37.62

306

3.3 Influence of operational conditions on MTBE removal

3.3.1 Effect of flow rate

Figure 2 shows the breakthrough curves at different flow rates of 0.5, 1 to 2 mL·min^{-1} in relation to pore volume and service time. As shown in Figure 2, the plots were closer to a classic S-shaped breakthrough curve at a lower flow rate (0.5 mL·min^{-1}), indicating a slower process and a higher adsorption capacity (32.89 mg·g^{-1}).

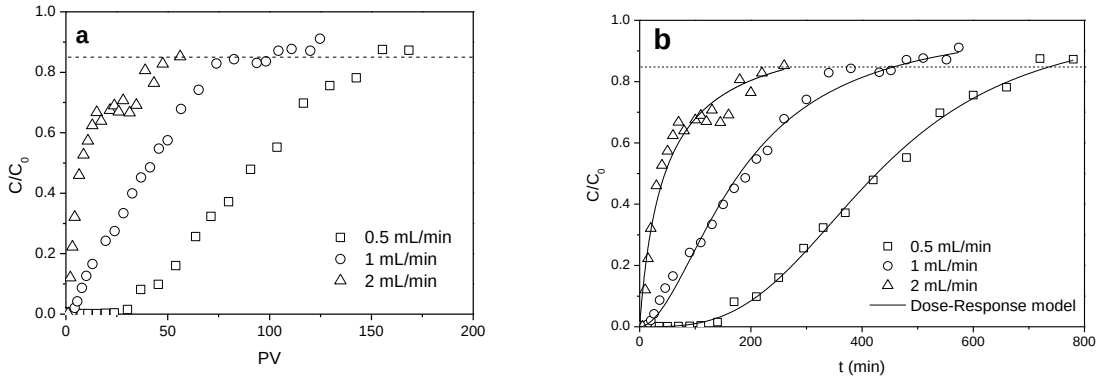

Figure 2 Breakthrough curves at different flow rates as a function of (a) pore volume (PV) and (b) time (t). (C_0=300 mg·L^{-1}, bed length=6 cm, ZSM-5 dosage=5%)

As the flow rate increased from 0.5 mL·min^{-1} to 2 mL·min^{-1}, the breakthrough time and saturation time decreased from 167.87 min to 2.08 min and from 740.18 min to 260.00 min, respectively. A lower column adsorption capacity was obtained at 25.85 mg·g^{-1} as shown in Table 3. This is due to the fact that the movement of MTBE is accelerated with an increase in the flow rate, which could cause insufficient residence time of MTBE in the column (Ozdemir et al., 2009; Salman et al., 2011). Similar agreement was found for the adsorption of nitrate on bio-inspired polydopamine coated zeolite and was explained by low residency in the column at high flow rate (Gouran-Orimi et al., 2018).

3.3.2 Effect of bed length

The breakthrough profiles at different bed lengths of 3 cm (1.03 g), 6 cm (2.05 g) and 9 cm (3.1 g) are shown in Figure 3. The decreasing bed length led to a faster breakthrough and saturation process, which resulted in earlier exhaustion of the bed. The increase in the breakthrough time could be attributed to the longer distance and moving time of the mass transfer zone between two ends of the column at a longer bed length (Salman et al., 2011), which was consistent with the calculated lengths of the mass transfer zone in Table 3. On the other hand, the increase in the bed length also led to the increasing mass of ZSM-5 and provided more adsorption sites for MTBE removal. It is noted that, as shown in Table 3, the increase in bed length gave rise to the increase in the total treated MTBE volume and saturation time in Figure 3b; however, the amounts of PVs through the column at saturation time were almost the same for various bed lengths in Figure 3a. This is due to that given the same flow rate and contaminant concentration, the adsorption capacity per unit bed length is constant.

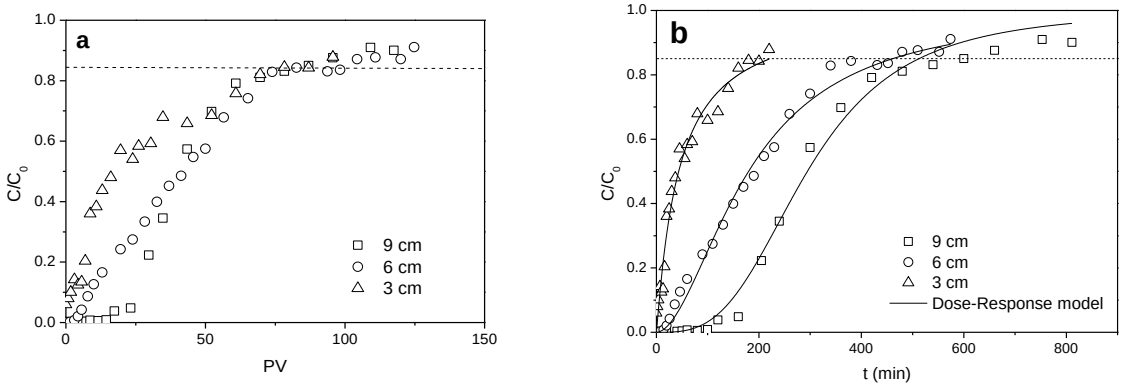

Figure 3 Breakthrough curves at different bed lengths as function of (a) pore volume (PV) and (b) time (t). (flow rate=1 mL·min^{-1}, C_0=300 mg·L^{-1}, ZSM-5 dosage=5%) (adapted from (Zhang et al., 2018a))

In addition, the BDST model was applied to produce the plots of Z versus t in Figure 4 for 5%, 20%, 50%, 60% and 85% saturation of the column with good linearity (R^2>0.9). The

parameters are calculated and listed in Table 4. With the increase of C/C_0 values from 5% (breakthrough point) to 85% (saturation point), the values of N_0 increased from 1787.80 $mg \cdot L^{-1}$ to 4646.93 $mg \cdot L^{-1}$, whereas those of K_{AB} decreased from 1.61×10^{-4} to 5.48×10^{-5} $L \cdot mg^{-1} \cdot min^{-1}$.

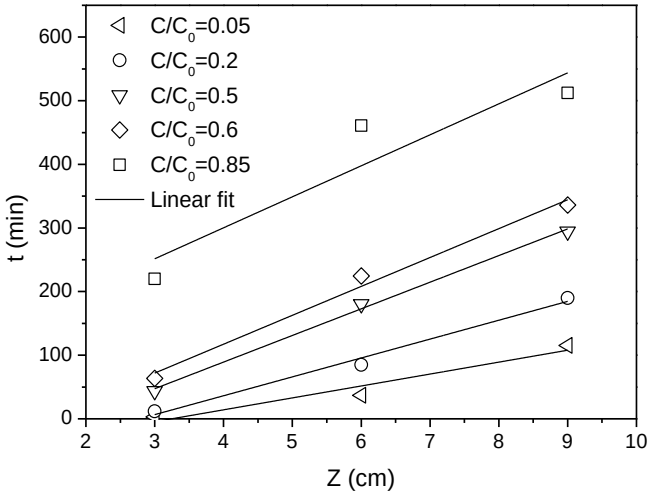

Figure 4 BDST lines at C/C_0 of 0.05, 0.2, 0.5, 0.6, 0.85 with different bed lengths (flow rate=1 $mL \cdot min^{-1}$, C_0=300 $mg \cdot L^{-1}$, ZSM-5 dosage=5%)

Table 4 Calculated parameters of the BDST model for MTBE adsorption on ZSM-5 in the fix-bed column tests

C/C_0	Equations	N_0 ($mg \cdot L^{-1}$)	k_{AB} ($L \cdot mg^{-1} \cdot min^{-1}$)	R^2
0.05	t=18.74Z-60.78	1787.80	1.61×10^{-4}	0.900
0.2	t=29.68Z-82.44	2831.47	5.61×10^{-5}	0.979
0.5	t=41.85Z-78.19	3992.49	0	0.995
0.85	t=48.71Z+105.44	4646.93	5.48×10^{-5}	0.755

The BDST model parameters are of great use for the scale-up of the adsorption process. For example, the groundwater velocities under natural gradient conditions are generally between

1 and 1000 m·year^{-1} (0.002-2 cm·min^{-1}) (Mackay et al., 1985), far lower than the flow rates adopted in this study. According to Equation (12) and (13), the BDST model can be employed to predict the adsorption efficiency and column performance under other operational conditions without further experimental runs (Han et al., 2009a; Vijayaraghavan and Prabu, 2006). Table 5 lists the predicted breakthrough time for a new flow rate (0.01 mL·min^{-1} or 0.003 cm·min^{-1}). Where $t_{c\ is}$ the predicted time and t_e is the observed time in the experiments.

Table 5 Breakthrough time prediction using BDST model at a new flow rate (ZSM-5 percentage=5%)

Operational conditions	C/C_0	New equations	t_c (min)	t_e (min)	RE[a]
Q'=0.5 mL·min^{-1}	0.05	t'=37.48Z-60.78	164.1	167.87	2.25%
Z=6 cm	0.2	t'=59.36Z-82.44	273.72	274.83	0.40%
C_0'=300 mg·L^{-1}	0.5	t'=83.70Z-78.19	424.01	427.09	0.72%
	0.85	t'=97.42Z+105.44	689.96	740.18	6.79%
Q'=0.01 mL·min^{-1}	0.05	t'=1874Z-60.78	11183.22		
Z=6 cm	0.2	t'=2968Z-82.44	17725.56		
C_0=300 mg·L^{-1}	0.5	t'=4185Z-78.19	25031.81		
	0.85	t'=4871Z+105.44	29331.44		

[a] Relative error

It was shown that the values of predicted time at a new flow rate were satisfactory with low relative errors. This indicates that the BDST model parameters in Table 4 can be employed to predict the column performance for the MTBE adsorption of ZSM-5 at different flow rates.

3.3.3 Effect of ZSM-5 dosage

The plots of effluent MTBE concentration versus PV and t at different ZSM-5 dosages are shown in Figure 5a and 5b, respectively.

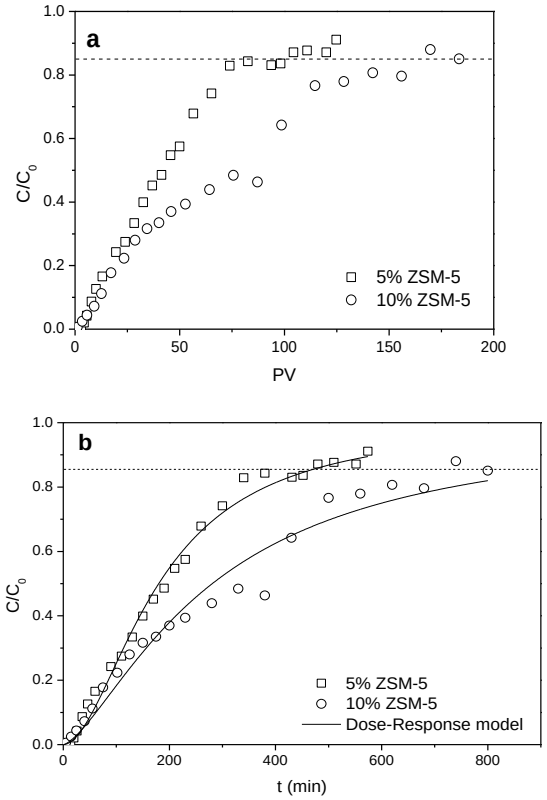

Figure 5 Breakthrough curves in fixed-bed columns with different ZSM-5 percentages as a function of (a) pore volume (PV) and (b) time (t). (C_0=300 mg·L^{-1}, bed length=6 cm, flow rate=1 mL·min^{-1})

The saturation time of the column with a higher ZSM-5 percentage (10%) was significantly longer and its breakthrough curve had a smaller gradient due to more available adsorption sites for MTBE removal in the column. However, the breakthrough time was almost unchanged with different ZSM-5 percentages.

3.3.4 Effect of inlet MTBE concentration

The effect of the influent MTBE concentration at 200, 300 and 400 mg·L^{-1} on the breakthrough profiles was analysed (Figure 6). It was observed that both the breakthrough time and saturation time decreased, and the slope of breakthrough curves between the breakthrough and saturate points, i.e. mass transfer zone (García-Mateos et al., 2015), became slightly steeper with the increase in the influent MTBE concentration. The steeper curve at higher inlet concentrations was an indicator of a smaller effluent volume whereas the extended breakthrough curve at lower inlet MTBE concentrations indicated that more solution was treated (Salman et al., 2011). This is because the higher concentration gradient at higher inlet MTBE concentrations caused a stronger mass transfer driving force (Goel et al., 2005) and faster solute transport in the column, leading to the quicker saturation of the adsorption sites on the ZSM-5 surface. The results in Table 3 show that the highest column adsorption capacity of 27.33 mg·g^{-1} was obtained at the inlet MTBE concentration of 400 mg·L^{-1}. Column tests at a low MTBE level (ug·L^{-1} level) will be explored in future.

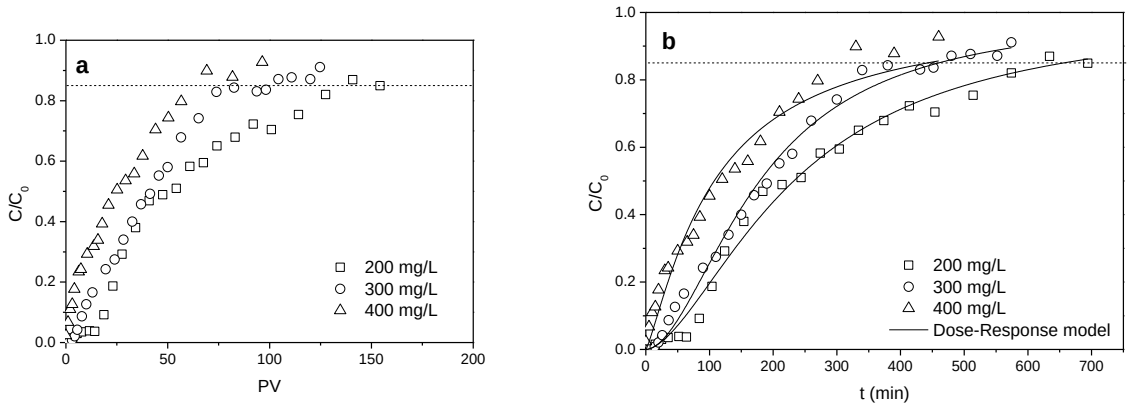

Figure 6 Breakthrough curves at inlet MTBE concentrations of 200, 300 and 400 mg·L^{-1} as function of (a) pore volume (PV) and (b) time (t) (bed length=6 cm, flow rate=1 mL·min^{-1}, ZSM-5=5%)

3.4 Predicted PRB thickness

The flow through thickness of a PRB is a main factor for the PRB design and can be calculated by Equation (13).

$$b = v \times t_w \quad (13)$$

where v is the velocity in the flow direction and t_w is the residence time. The residence time (half-life, t_w) was determined at 99.9% of the respective equilibrium MTBE removal using the best-fitting pseudo-second-order model in our previous study (Zhang et al., 2018) combined with the Solver function in MS Excel (Cai et al., 2018; Gavaskar et al., 2000). The residence time at different initial MTBE concentrations and predicted PRB thicknesses at a nominal groundwater velocity of 0.18 cm·h^{-1} (equivalent to 0.01 mL·min^{-1} pump rate in this study) are listed in Table 6. For example, the predicted PRB flow through thickness was found to be 114.85 cm for 99.9% MTBE removal at an inlet MTBE concentration of 300 mg·L^{-1}.

Table 6 Predicted residence time (h) and PRB thickness (cm) (v=0.18 cm·h^{-1})

Initial MTBE concentration (mg·L^{-1})	100	150	300	600
Residence time (h)	122.62	456.26	638.06	683.11
Thickness (cm)	22.07	82.13	114.85	122.96

There are some limitations of this study, such as (i) the inaccuracy of using batch tests for calculating residence time instead of calculating half-life of MTBE in the column tests; (ii) the use of deionised water without considering the NOM (nature organic matter) and other contaminants in the natural underground water, and (iii) the relatively high flow rate used. More advance column design and selection of a wider range of flow rates will be conducted in future studies to enable more accurate calculations.

Various remediation techniques have been applied to treat MTBE contaminated groundwater, such as classical (Xu et al., 2004) and electrochemical Fenton treatment (Hong et al., 2007), biodegradation by microorganism (Bradley et al., 1999), pump-and-treat, phytoremediation (Hong et al., 2001), PRBs (Obiri-Nyarko et al., 2014), in-situ chemical oxidation (Krembs et al., 2010), etc. The choice of remediation techniques depends on many factors, such as the physiochemical properties of treating agents, site characterization, concentrations of MTBE and other contaminates, and PRB is a promising in-situ groundwater remediation technique due to its low-cost. The PRB treatment of MTBE contaminated groundwater with ZSM-5 as the reactive medium is sustainable due to the adsorption of MTBE onto ZSM-5 without precipitation which may cause clogging and reduce the permeability and removal efficiency of PRBs (Zhou et al., 2014).

3.5 Regeneration study

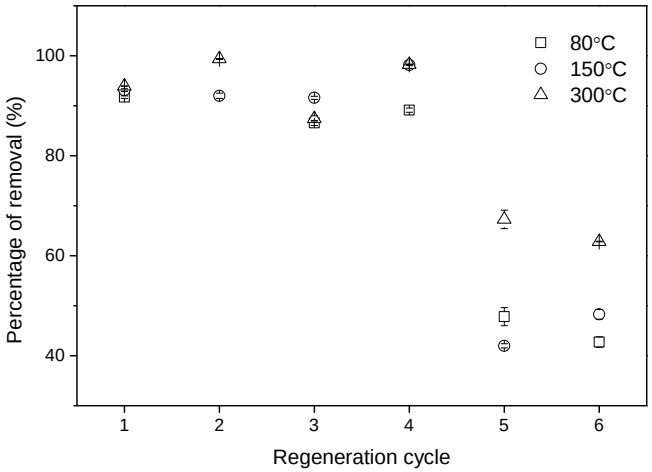

Figure 7 The MTBE removal percentage by ZSM-5 after 6 regeneration cycles

In order to estimate the reusability of ZSM-5, the effect of repeated heat treatment at different temperatures on the MTBE adsorption onto regenerated ZSM-5 was investigated and shown in Figure 7. It was observed that there were no apparent changes in adsorption effects up to

four regeneration cycles at all temperatures and the regeneration at higher temperature slightly increased the removal percentage. The abnormal value at the second cycle at 80 °C was not included due to operating error. However, after 6 regeneration cycles, the removal percentage decreased to ~67% at 300 °C compared with ~47% and ~52% for 80 °C and 150 °C, respectively. Therefore, ZSM-5 displays good regeneration potential compared with modified activated carbon (~18% after 6 cycles) and iron oxide coated zeolites (<6% after 3 cycles) (Ania et al., 2004; Han et al., 2009b). It should be noted that sand or other medium in PRBs should be heated with ZSM-5 in the practical application, and the vaporized MTBE could be collected and treated to avoid secondary pollution.

4. Conclusions

Fixed-bed column tests were combined with breakthrough curve modelling to describe the breakthrough curves and evaluate the adsorption performance under different operational conditions. The regeneration characteristics of ZSM-5 were also discussed. The conclusions are as follows:

(1) The results of both the regeneration tests and fixed-bed column tests show that ZSM-5 is an effective reactive medium in PRBs for MTBE contaminated groundwater remediation.

(2) The Dose-Response model was found to best describe the breakthrough curves compared with the Logit method, Adams-Bohart model, Thomas model and Yoon-Nelson model.

(3) The column adsorption capacity is ~31.85 $mg \cdot g^{-1}$ at a 6 cm bed length, 1 $mL \cdot min^{-1}$ flow rate, 300 $mg \cdot L^{-1}$ initial MTBE concentration and 5% ZSM-5 percentage.

(4) The maximum adsorption capacity increased with the increase of bed length and the decrease of flow rate and MTBE concentration from the Dose-Response model, while the adsorption capacity decreased with a higher ZSM-5 dosage due to the underestimate of

adsorption capacity caused by the fact that the ZSM-5 powder in the column may be more likely to run away with the MTBE flow with a higher ZSM-5 dosage.

(5) The kinetic parameters obtained from the BDST model can be employed to predict the dynamic behaviour of columns at new flow rates.

(6) The adsorption capacity of regenerated ZSM-5 remains satisfactory (>85%) after up to four regeneration cycles at 80, 150 and 300 °C and regeneration at higher temperatures performed slightly better.

Acknowledgements

The first author would like to thank China Scholarship Council (CSC) for providing the PhD studentship, and the third author is grateful to the Killam Trusts of Canada for the Izaak Walton Killam Memorial Postdoctoral Fellowship.

References

Abu-Lail, L., Bergendahl, J.A., Thompson, R.W., 2010. Adsorption of methyl tertiary butyl ether on granular zeolites: Batch and column studies. J. Hazard. Mater. 178, 363–369. https://doi.org/10.1016/j.jhazmat.2010.01.088

Adak, A., Pal, A., 2006. Removal of phenol from aquatic environment by SDS-modified alumina: Batch and fixed bed studies. Sep. Purif. Technol. 50, 256–262. https://doi.org/10.1016/J.SEPPUR.2005.11.033

Al-Tabbaa, A., Liska, M., 2012. Soil mix remediation technology (SMiRT) final technical summary report (confidential).

Anderson, M.A., 2000. Removal of MTBE and other organic contaminants from water by sorption to high silica zeolites. Environ. Sci. Technol. 34, 725–727. https://doi.org/10.1021/es990390t

Ania, C.O., Menéndez, J.A., Parra, J.B., Pis, J.J., 2004. Microwave-induced regeneration of activated carbons polluted with phenol. A comparison with conventional thermal regeneration, in: Carbon. https://doi.org/10.1016/j.carbon.2004.01.010

Ayoob, S., Gupta, A.K., 2007. Sorptive response profile of an adsorbent in the defluoridation of drinking water. Chem. Eng. J. https://doi.org/10.1016/j.cej.2007.02.013

Bohart, G.S., Adams, E.Q., 1920. Some aspects of the behavior of charcoal with respect to chlorine. J. Am. Chem. Soc. 42, 523–544. https://doi.org/10.1021/ja01448a018

Bradley, P.M., Landmeyer, J.E., Chapelle, F.H., 1999. Aerobic mineralization of MTBE and tert-butyl alcohol by stream-bed sediment microorganisms. Environ. Sci. Technol. https://doi.org/10.1021/es990062t

Cai, Q., Turner, B.D., Sheng, D., Sloan, S., 2018. Application of kinetic models to the design of a calcite permeable reactive barrier (PRB) for fluoride remediation. Water Res. https://doi.org/10.1016/j.watres.2017.11.046

Calero, M., Hernáinz, F., Blázquez, G., Tenorio, G., Martín-Lara, M.A., 2009. Study of Cr (III) biosorption in a fixed-bed column. J. Hazard. Mater. 171, 886–893. https://doi.org/10.1016/j.jhazmat.2009.06.082

Cappai, G., De Gioannis, G., Muntoni, A., Spiga, D., Zijlstra, J.J.P., 2012. Combined use of a transformed red mud reactive barrier and electrokinetics for remediation of Cr/As contaminated soil. Chemosphere 86, 400–408. https://doi.org/10.1016/J.CHEMOSPHERE.2011.10.053

Centi, G., Grande, A., Perathoner, S., 2002. Catalytic conversion of MTBE to biodegradable chemicals in contaminated water, in: Catalysis Today. https://doi.org/10.1016/S0920-5861(02)00046-9

Centi, G., Perathoner, S., 2003. Remediation of water contamination using catalytic technologies. Appl. Catal. B Environ. https://doi.org/10.1016/S0926-3373(02)00198-4

Chan, M.S.M., Lynch, R.J., 2003. Photocatalytic degradation of aqueous methyl-tert-butyl-ether (MTBE) in a supported-catalyst reactor. Environ. Chem. Lett. 1, 157–160. https://doi.org/10.1007/s10311-003-0037-4

Cruz Viggi, C., Pagnanelli, F., Cibati, A., Uccelletti, D., Palleschi, C., Toro, L., 2010. Biotreatment and bioassessment of heavy metal removal by sulphate reducing bacteria in fixed bed reactors. Water Res. 44, 151–158. https://doi.org/10.1016/j.watres.2009.09.013

Dorado, A.D., Gamisans, X., Valderrama, C., Solé, M., Lao, C., 2014. Cr(III) removal from aqueous solutions: A straightforward model approaching of the adsorption in a fixed-bed column. J. Environ. Sci. Heal. - Part A Toxic/Hazardous Subst. Environ. Eng. 49, 179–186. https://doi.org/10.1080/10934529.2013.838855

García-Mateos, F.J., Ruiz-Rosas, R., Marqués, M.D., Cotoruelo, L.M., Rodríguez-Mirasol, J., Cordero, T., 2015. Removal of paracetamol on biomass-derived activated carbon:

536 Modeling the fixed bed breakthrough curves using batch adsorption experiments. Chem.
537 Eng. J. 279, 18–30. https://doi.org/10.1016/j.cej.2015.04.144
538 Gavaskar, A., Gupta, N., Sass, B., Janosy, R., Hicks, J., 2000. Design guidance for
539 application of Permeable Reactive Barriers for groundwater remediation.
540 Gavaskar, A.R., 1999. Design and construction techniques for permeable reactive barriers. J.
541 Hazard. Mater. 68, 41–71. https://doi.org/10.1016/S0304-3894(99)00031-X
542 Goel, J., Kadirvelu, K., Rajagopal, C., Kumar Garg, V., 2005. Removal of lead(II) by
543 adsorption using treated granular activated carbon: Batch and column studies. J. Hazard.
544 Mater. 125, 211–220. https://doi.org/10.1016/j.jhazmat.2005.05.032
545 Gouran-Orimi, R., Mirzayi, B., Nematollahzadeh, A., Tardast, A., 2018. Competitive
546 adsorption of nitrate in fixed-bed column packed with bio-inspired polydopamine coated
547 zeolite. J. Environ. Chem. Eng. 6, 2232–2240. https://doi.org/10.1016/j.jece.2018.01.049
548 Han, R., Ding, D., Xu, Y., Zou, W., Wang, Y., Li, Y., Zou, L., 2008. Use of rice husk for the
549 adsorption of congo red from aqueous solution in column mode. Bioresour. Technol. 99,
550 2938–2946. https://doi.org/10.1016/j.biortech.2007.06.027
551 Han, R., Wang, Y., Zhao, X., Wang, Y., Xie, F., Cheng, J., Tang, M., 2009a. Adsorption of
552 methylene blue by phoenix tree leaf powder in a fixed-bed column: Experiments and
553 prediction of breakthrough curves. Desalination 245, 284–297.
554 https://doi.org/10.1016/j.desal.2008.07.013
555 Han, R., Zou, L., Zhao, X., Xu, Y., Xu, F., Li, Y., Wang, Y., 2009b. Characterization and
556 properties of iron oxide-coated zeolite as adsorbent for removal of copper(II) from
557 solution in fixed bed column. Chem. Eng. J. 149, 123–131.
558 https://doi.org/10.1016/j.cej.2008.10.015
559 Hong, M.S., Farmayan, W.F., Dortch, I.J., Chiang, C.Y., McMillan, S.K., Schnoor, J.L., 2001.
560 Phytoremediation of MTBE from a groundwater plume. Environ. Sci. Technol.

561 https://doi.org/10.1021/es001911b
562 Hong, S., Zhang, H., Duttweiler, C.M., Lemley, A.T., 2007. Degradation of methyl tertiary-
563 butyl ether (MTBE) by anodic Fenton treatment. J. Hazard. Mater.
564 https://doi.org/10.1016/j.jhazmat.2006.12.030
565 Hou, D., Al-Tabbaa, A., Luo, J., 2014. Assessing effects of site characteristics on remediation
566 secondary life cycle impact with a generalised framework. J. Environ. Plan. Manag. 57,
567 1083–1100. https://doi.org/10.1080/09640568.2013.863754
568 Hutchins, R., 1973. New method simplifies design of activated-carbon systems. Chem. Eng.
569 80, 133–138.
570 Jha, B., Singh, D.N., 2016. Fly ash zeolites, Advanced Structured Materials. Springer
571 Singapore, Singapore. https://doi.org/10.1007/978-981-10-1404-8
572 Katsou, E., Malamis, S., Tzanoudaki, M., Haralambous, K.J., Loizidou, M., 2011.
573 Regeneration of natural zeolite polluted by lead and zinc in wastewater treatment
574 systems. J. Hazard. Mater. 189, 773–786. https://doi.org/10.1016/j.jhazmat.2010.12.061
575 Krembs, F.J., Siegrist, R.L., Crimi, M.L., Furrer, R.F., Petri, B.G., 2010. ISCO for
576 groundwater remediation: Analysis of field applications and performance. Gr. Water
577 Monit. Remediat. https://doi.org/10.1111/j.1745-6592.2010.01312.x
578 Levchuk, I., Bhatnagar, A., Sillanpää, M., 2014. Overview of technologies for removal of
579 methyl tert-butyl ether (MTBE) from water. Sci. Total Environ.
580 https://doi.org/10.1016/j.scitotenv.2014.01.037
581 Lindsey, B.D., Ayotte, J.D., Jurgens, B.C., Desimone, L.A., 2017. Using groundwater age
582 distributions to understand changes in methyl tert-butyl ether (MtBE) concentrations in
583 ambient groundwater, northeastern United States. Sci. Total Environ. 579, 579–587.
584 https://doi.org/10.1016/j.scitotenv.2016.11.058
585 Mackay, D.M., Roberts, P. V., Cherry, J.A., 1985. Transport of organic contaminants in

groundwater. Environ. Sci. Technol. 19, 384–392. https://doi.org/10.1021/es00135a001

Mancini, E.R., Steen, A., Rausina, G.A., Wong, D.C.L., Arnold, W.R., Gostomski, F.E., Davies, T., Hockett, J.R., Stubblefield, W.A., Drottar, K.R., Springer, T.A., Errico, P., 2002. MTBE ambient water quality criteria development: A public/private partnership. Environ. Sci. Technol. 36, 125–129. https://doi.org/10.1021/es002059b

Martucci, A., Braschi, I., Bisio, C., Sarti, E., Rodeghero, E., Bagatin, R., Pasti, L., 2015. Influence of water on the retention of methyl tertiary-butyl ether by high silica ZSM-5 and Y zeolites: a multidisciplinary study on the adsorption from liquid and gas phase. RSC Adv. 5, 86997–87006. https://doi.org/10.1039/C5RA15201A

Masad, E., Taha, R., Ho, C., Papagiannakis, T., 1996. Engineering properties of tire/soil mixtures as a lightweight fill material. Geotech. Test. Journal, 19, 297–304. https://doi.org/10.1520/GTJ10355J

Mohebali, S., 2013. Degradation of methyl t-butyl ether (MTBE) by photochemical process in nanocrystalline TiO2 slurry: Mechanism, by-products and carbonate ion effect. J. Environ. Chem. Eng. 1, 1070–1078. https://doi.org/10.1016/j.jece.2013.08.022

Obiri-Nyarko, F., Grajales-Mesa, S.J., Malina, G., 2014. An overview of permeable reactive barriers for in situ sustainable groundwater remediation. Chemosphere. https://doi.org/10.1016/j.chemosphere.2014.03.112

Oulman, C., 1980. The logistic curve as a model for carbon bed design. J. AWWA 72, 50–53.

Ozdemir, O., Turan, M., Turan, A.Z., Faki, A., Engin, A.B., 2009. Feasibility analysis of color removal from textile dyeing wastewater in a fixed-bed column system by surfactant-modified zeolite (SMZ). J. Hazard. Mater. 166, 647–654. https://doi.org/10.1016/j.jhazmat.2008.11.123

Pascoe, W.E., 1992. Catalysis of organic reactions. Marcel Dekker, New York.

Reuter, J.E., Allen, B.C., Richards, R.C., Pankow, J.F., Goldman, C.R., Roger L. Schol, A.,

611 Seyfried, J.S., 1998. Concentrations, sources, and fate of the gasoline oxygenate Methyl
612 tert-Butyl Ether (MTBE) in a multiple-use lake. Environ. Sci. Technol. 32, 3666–3672.
613 https://doi.org/10.1021/ES9805223
614 Sağ, Y., Aktay, Y., 2001. Application of equilibrium and mass transfer models to dynamic
615 removal of Cr(VI) ions by Chitin in packed column reactor. Process Biochem. 36, 1187–
616 1197. https://doi.org/10.1016/S0032-9592(01)00150-9
617 Salman, J., Njoku, V., Hameed, B., 2011. Batch and fixed-bed adsorption of 2, 4-
618 dichlorophenoxyacetic acid onto oil palm frond activated carbon. Chem. Eng. J. 174,
619 33–40.
620 Shah, I.K., Pre, P., Alappat, B.J., 2014. Effect of thermal regeneration of spent activated
621 carbon on volatile organic compound adsorption performances. J. Taiwan Inst. Chem.
622 Eng. 45, 1733–1738. https://doi.org/10.1016/J.JTICE.2014.01.006
623 Thomas, H., 1944. Heterogeneous ion exchange in a flowing system. J. Am. Chem. Soc. 66,
624 1664–1666.
625 Thomas, H.C., 1948. Chromatography: A problem in kinetics. Ann. N. Y. Acad. Sci. 49,
626 161–182. https://doi.org/10.1111/j.1749-6632.1948.tb35248.x
627 Vijayaraghavan, K., Prabu, D., 2006. Potential of Sargassum wightii biomass for copper(II)
628 removal from aqueous solutions: Application of different mathematical models to batch
629 and continuous biosorption data. J. Hazard. Mater. 137, 558–564.
630 https://doi.org/10.1016/j.jhazmat.2006.02.030
631 Wang, S., Zhu, Z.H., 2006. Characterisation and environmental application of an Australian
632 natural zeolite for basic dye removal from aqueous solution. J. Hazard. Mater. 136, 946–
633 952. https://doi.org/10.1016/j.jhazmat.2006.01.038
634 Wei, Y.X., Ye, Z.F., Wang, Y.L., Ma, M.G., Li, Y.F., 2011. Enhanced ammonia nitrogen
635 removal using consistent ammonium exchange of modified zeolite and biological

636 regeneration in a sequencing batch reactor process. Environ. Technol. 32, 1337–1343.
637 https://doi.org/10.1080/09593330.2010.536784
638 Xin, S., Zeng, Z., Zhou, X., Luo, W., Shi, X., Wang, Q., Deng, H., Du, Y., 2017. Recyclable
639 Saccharomyces cerevisiae loaded nanofibrous mats with sandwich structure constructing
640 via bio-electrospraying for heavy metal removal. J. Hazard. Mater. 324, 365–372.
641 https://doi.org/10.1016/j.jhazmat.2016.10.070
642 Xu, X.R., Zhao, Z.Y., Li, X.Y., Gu, J.D., 2004. Chemical oxidative degradation of methyl
643 tert-butyl ether in aqueous solution by Fenton's reagent. Chemosphere.
644 https://doi.org/10.1016/j.chemosphere.2003.11.017
645 Yan, G., Viraraghavan, T., Chen, M., 2001. A new model for heavy metal removal in a
646 biosorption column. Adsorpt. Sci. Technol. 19, 25–43.
647 https://doi.org/10.1260/0263617011493953
648 Yoon, Y.H., 1984. Application of gas adsorption kinetics. A Theor. Model Respir. Cart. Serv.
649 life 45, 509–516.
650 Zhang, Y., Jin, F., Lynch, R., Al-Tabbaa, A., 2018a. Breakthrough curve modelling of ZSM-
651 5 zeolite packed fixed-bed columns for the removal of MTBE, in: The 8th International
652 Congress on Environmental Geotechnics (Forthcoming).
653 Zhang, Y., Jin, F., Shen, Z., Lynch, R., Al-Tabbaa, A., 2018b. Kinetic and equilibrium
654 modelling of MTBE (methyl tert-butyl ether) adsorption on ZSM-5 zeolite: Batch and
655 column studies. J. Hazard. Mater. 347, 461–469.
656 https://doi.org/10.1016/J.JHAZMAT.2018.01.007
657 Zhou, D., Li, Y., Zhang, Y., Zhang, C., Li, X., Chen, Z., Huang, J., Li, X., Flores, G., Kamon,
658 M., 2014. Column test-based optimization of the permeable reactive barrier (PRB)
659 technique for remediating groundwater contaminated by landfill leachates. J. Contam.
660 Hydrol. https://doi.org/10.1016/j.jconhyd.2014.09.003

Figure
Click here to download Figure: Figures.docx

Figures

Figure 1 The schematic of the fixed-bed column set-up in this study

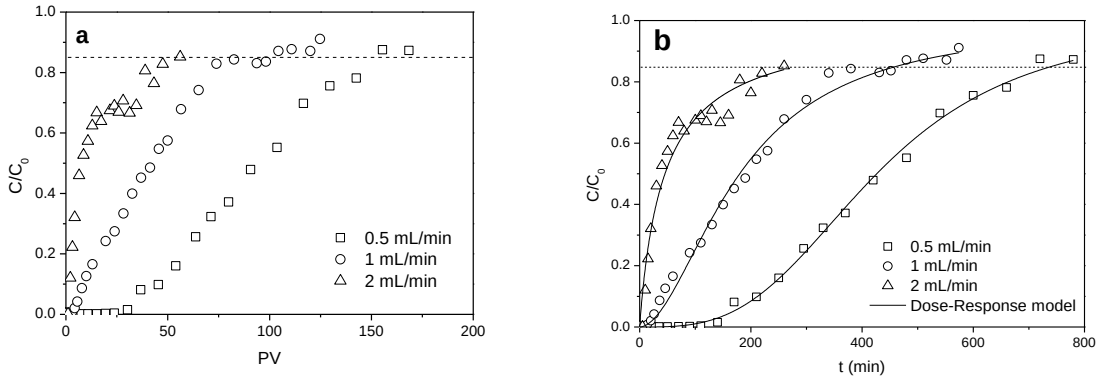

Figure 2 Breakthrough curves at different flow rates as a function of (a) pore volume (PV) and (b) time (t). (C_0=300 mg·L^{-1}, bed length=6 cm, ZSM-5 dosage=5%)

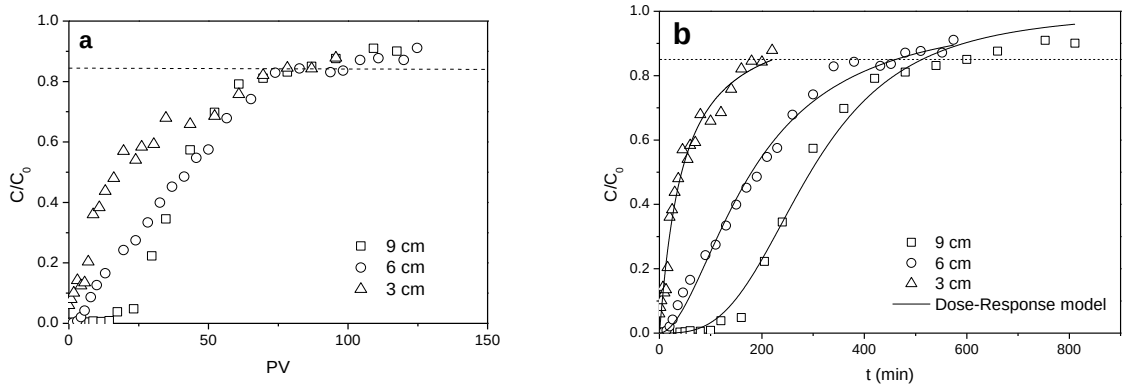

Figure 3 Breakthrough curves at different bed lengths as function of (a) pore volume (PV) and (b) time (t). (flow rate=1 mL·min^{-1}, C_0=300 mg·L^{-1}, ZSM-5 dosage=5%) (adapted from (Zhang et al., 2018a))

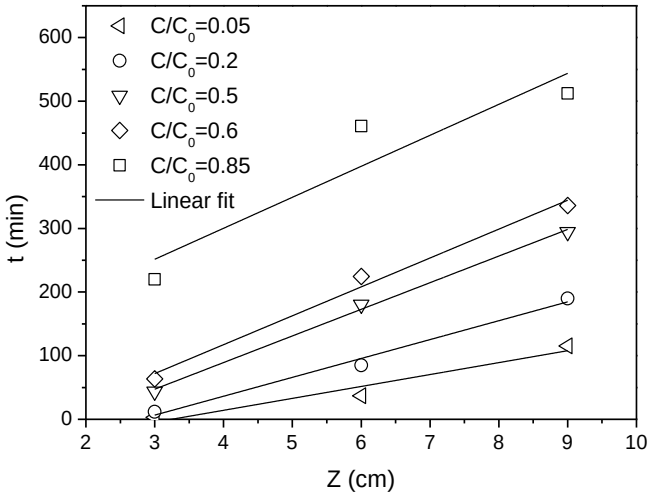

Figure 4 BDST lines at C/C_0 of 0.05, 0.2, 0.5, 0.6, 0.85 with different bed lengths (flow rate=1 $mL \cdot min^{-1}$, C_0=300 $mg \cdot L^{-1}$, ZSM-5 dosage=5%)

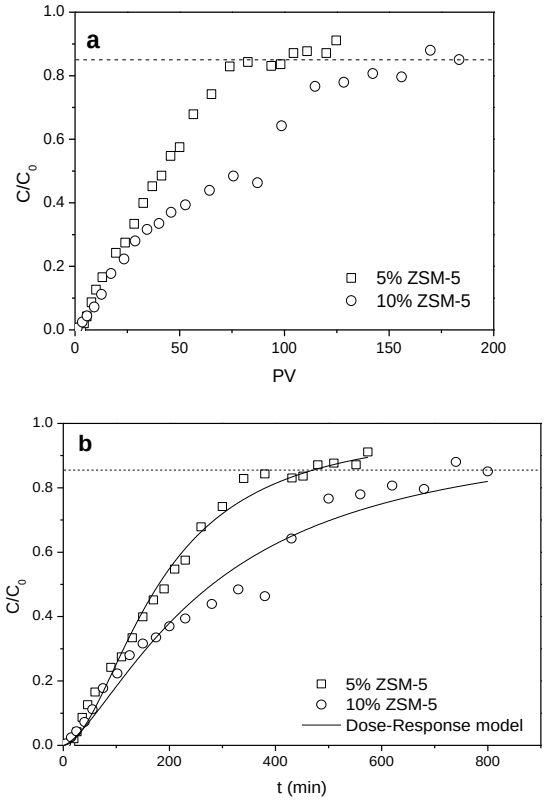

Figure 5 Breakthrough curves in fixed-bed columns with different ZSM-5 percentages as a function of (a) pore volume (PV) and (b) time (t). (C_0=300 mg·L^{-1}, bed length=6 cm, flow rate=1 mL·min^{-1})

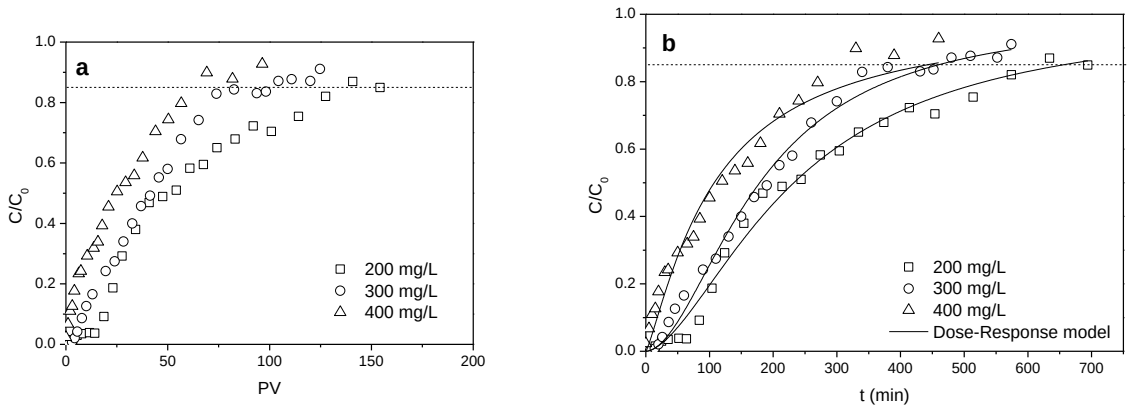

Figure 6 Breakthrough curves at inlet MTBE concentrations of 200, 300 and 400 mg·L^{-1} as function of (a) pore volume (PV) and (b) time (t) (bed length=6 cm, flow rate=1 mL·min^{-1}, ZSM-5=5%)

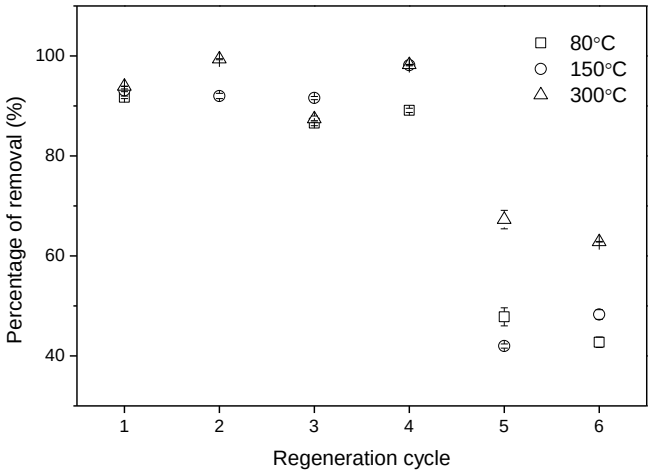

Figure 7 The MTBE removal percentage by ZSM-5 after 6 regeneration cycles

Tables

Table 1 Operational variables for fixed-bed column tests

Test No.	Influencing factors	Flow rate ($mL \cdot min^{-1}$)	Bed length (cm)	m_{ZSM-5} (g)	ZSM-5 (%)	C_0 (MTBE) ($mg \cdot L^{-1}$)	Porosity
F0.5	Flow rate	0.5	6	2.05	5	300	0.25
C	Flow rate	1	6	2.05	5	300	0.24
F2	Flow rate	2	6	2.05	5	300	0.24
B3	Bed length	1	3	1.03	5	300	0.24
C	Bed length	1	6	2.05	5	300	0.24
B9	Bed length	1	9	3.08	5	300	0.24
C	ZSM-5 dosage	1	6	2.05	5	300	0.24
Z10	ZSM-5 dosage	1	6	4.50	10	300	0.23
M200	MTBE concentration	1	6	2.07	5	200	0.24
C	MTBE concentration	1	6	2.05	5	300	0.24
M400	MTBE concentration	1	6	2.03	5	400	0.25

Table 2 Dose-Response model parameters for the MTBE adsorption on ZSM-5 under different operational conditions

Variables	Test No.	a	b (mL)	q_0 ($mg \cdot g^{-1}$)	R^2
Flow rate	C	1.84	179.88	26.32	0.993
	F0.5	3.14	213.16	31.19	0.997
	F2	0.95	90.99	13.32	0.959
Bed length	C	1.84	179.88	26.32	0.993
	B3	1.06	43.46	12.66	0.997
	B9	3.14	294.63	28.70	0.991
ZSM-5 percentage	C	1.84	179.88	26.32	0.993
	Z10	1.45	280.78	18.72	0.971
Initial MTBE concentration	C	1.84	179.88	26.32	0.993
	M200	1.67	232.38	22.45	0.989
	M400	1.23	107.34	21.15	0.969

Table 3 Parameters of breakthrough curves for MTBE adsorption on ZSM-5 in fixed-bed columns under different operational conditions

Test No.	C	F0.5	F2	B3	B9	Z10	M200	M400
t_b (min)	36.77	167.87	2.08	2.86	115.28	36.84	40.29	10.13
t_s (min)	460.81	740.18	260.00	220.00	512.25	919.75	655.79	442.04
$MTZ = \frac{Z(t_s - t_b)}{t_s}$ (cm)	5.52	4.64	5.95	2.96	6.97	5.76	5.63	5.86
$m_{adsorb} = \frac{Q}{1000}\int_{t=0}^{t=t_{total}}(C_0 - C)dt$ (mg)	65.30	67.42	52.99	23.01	93.23	114.99	52.77	66.52
$m_{total} = \frac{C_0 Q t_{total}}{1000}$ (mg)	138.24	111.03	156.00	66.00	153.68	275.93	131.16	176.82
$q_e = \frac{m_{adsorb}}{m_{zsm-5}}$ (mg·g^{-1})	31.85	32.89	25.85	22.34	30.27	25.55	25.49	32.77
$C_e = \frac{1000(m_{total} - m_{adsorb})}{Q t_{total}}$ (mg·L^{-1})	158.29	117.82	198.10	195.42	118.00	174.98	119.53	249.52
$R = \frac{100 m_{adsorb}}{m_{total}}$ (%)	47.24	60.73	33.97	34.86	60.67	41.67	40.23	37.62

Table 4 Calculated parameters of the BDST model for MTBE adsorption on ZSM-5 in the fix-bed column tests

C/C_0	Equations	N_0 ($mg \cdot L^{-1}$)	k_{AB} ($L \cdot mg^{-1} \cdot min^{-1}$)	R^2
0.05	t=18.74Z-60.78	1787.80	1.61×10^{-4}	0.900
0.2	t=29.68Z-82.44	2831.47	5.61×10^{-5}	0.979
0.5	t=41.85Z-78.19	3992.49	0	0.995
0.85	t=48.71Z+105.44	4646.93	5.48×10^{-5}	0.755

Table 5 Breakthrough time prediction using BDST model at a new flow rate (ZSM-5 percentage=5%)

Operational conditions	C/C_0	New equations	t_c (min)	t_e (min)	RE[a]
Q'=0.5 mL·min^{-1}	0.05	t'=37.48Z-60.78	164.1	167.87	2.25%
Z=6 cm	0.2	t'=59.36Z-82.44	273.72	274.83	0.40%
C_0'=300 mg·L^{-1}	0.5	t'=83.70Z-78.19	424.01	427.09	0.72%
	0.85	t'=97.42Z+105.44	689.96	740.18	6.79%
Q'=0.01 mL·min^{-1}	0.05	t'=1874Z-60.78	11183.22		
Z=6 cm	0.2	t'=2968Z-82.44	17725.56		
C_0=300 mg·L^{-1}	0.5	t'=4185Z-78.19	25031.81		
	0.85	t'=4871Z+105.44	29331.44		

[a] Relative error

Table 6 Predicted residence time (h) and PRB thickness (cm) (v=0.18 cm·h^{-1})

Initial MTBE concentration (mg·L^{-1})	100	150	300	600
Residence time (h)	122.62	456.26	638.06	683.11
Thickness (cm)	22.07	82.13	114.85	122.96

*Title Page

Adsorption of Methyl tert-butyl ether (MTBE) onto ZSM-5 zeolite: Fixed-bed column tests, breakthrough curve modelling and regeneration

Yunhui Zhang[a*]; Fei Jin[b]; Zhengtao Shen[c]; Fei Wang[d]; Rod Lynch[a]; Abir Al-Tabbaa[a]

[a]Department of Engineering, University of Cambridge, Cambridge, CB2 1PZ, United Kingdom

[b]School of Engineering, University of Glasgow, Glasgow, G12 8QQ, United Kingdom

[c]Department of Earth and Atmospheric Sciences, University of Alberta, Edmonton T6G 2E3, Canada

[d]Institute of Geotechnical Engineering, School of Transportation, Southeast University, Nanjing, 210096, China

AUTHOR INFORMATION

***Corresponding Author**

Tel: +44- (0) 7821464199

E-mail address: yz485@cam.ac.uk.

Supplementary Material

Click here to download Supplementary Material: Supplementary Material.docx

***Highlights (3 to 5 bullet points (maximum 85 characters including spaces per bullet point)**

Highlights

- ZSM-5 is evaluated on its removal for MTBE in fixed-bed column tests.
- Dose-Response model was found to best describe the breakthrough curves.
- The removal capacity is ~31.85 $mg \cdot g^{-1}$ in fixed-bed column tests.
- Parameters from BDST model can predict breakthrough curves at a new flow rate.
- ZSM-5 is effective and recyclable for MTBE contaminated groundwater remediation.